The Cryosphere Discuss., 7, 267–319, 2013
www.the-cryosphere-discuss.net/7/267/2013/
doi:10.5194/tcd-7-267-2013

The Cryosphere Discussions

Area and volume loss of the glaciers in the Ortles-Cevedale group (Eastern Italian Alps): controls and imbalance of the remaining glaciers

L. Carturan[1], R. Filippi[2,3,4,*], R. Seppi[5], P. Gabrielli[3,6], C. Notarnicola[2], L. Bertoldi[7], F. Paul[8], P. Rastner[8], F. Cazorzi[9], R. Dinale[10], and G. Dalla Fontana[1]

[1]Department of Land, Environment, Agriculture and Forestry, University of Padova, Agripolis, Viale dell'Università 16, 35020 Legnaro, Padova, Italy
[2]Institute for Applied Remote Sensing, EURAC, Viale Druso 1, 39100 Bolzano, Italy
[3]Byrd Polar Research Center, The Ohio State University, 108 Scott Hall, 1090 Carmack Road, Columbus, Ohio 43210-1002, USA
[4]Museo delle Scienze, Via Calepina 14, 38122, Trento, Italy
[5]Department of Earth and Environmental Sciences, University of Pavia, Via Ferrata 1, 27100, Pavia, Italy
[6]School of Earth Science, The Ohio State University, 275 Mendenhall Laboratory, 125 South Oval Mall, Columbus, Ohio 43210, USA
[7]Chartagena, aerial analysis, Via Maccani 211, 38121, Trento, Italy

[8]Department of Geography, University of Zurich, – Irchel Winterthurerstr. 190, 8057 Zurich, Switzerland
[9]Department of Agriculture and Environmental Science, University of Udine, Via delle Scienze 208, 33100 Udine, Italy
[10]Ufficio Idrografico – Provincia Autonoma di Bolzano, Via Mendola 33, 39100 Bolzano, Italy
*deceased

Received: 14 November 2012 – Accepted: 28 December 2012 – Published: 21 January 2013

Correspondence to: L. Carturan (luca.carturan@unipd.it)

Published by Copernicus Publications on behalf of the European Geosciences Union.

TCD
7, 267–319, 2013

Abstract

A widespread loss of glacier area and volume was observed in the European Alps since the 1980s. Besides differences among various regions of the Alps, different responses characterize neighboring glaciers within the same region. In this study we describe the glacier changes in the Ortles-Cevedale group, the largest glacierized area in the Italian Alps. We characterize the drivers, the spatial variability and the main factors controlling the current loss of ice in this region by comparing glacier extents and snow covered areas derived from Landsat images acquired in 1987 and 2009. Glacier outlines were obtained from a band ratio with manual corrections and snow was classified from a near infrared image after topographic correction. The total glacierized area shrank by 23 % in this period, with no significant changes in the mean altitude of the glaciers. The snowline is now 240 m higher than in the 1960s and 1970s. From the snow covered area of 2009, which fairly represents the extent of the accumulation areas over the last decade, we estimate that about 50 % of the remaining glacier surfaces have to melt away to re-establish equilibrium with present climatic conditions. The average geodetic mass budget rate, calculated for 112 ice bodies by differencing two Digital Terrain Models (DTMs), ranged from −0.15 to −1.50 m w.e. a^{-1}, averaging −0.68 m w.e. a^{-1}. A correlation analysis of mass budgets vs. topographic variables confirmed the important role of the hypsometry in controlling area and volume loss of larger glaciers, while a higher variability characterizes smaller glaciers and glacierets, likely due to the increasing importance of local topo-climatic conditions.

1 Introduction

The response of glaciers to climatic fluctuations is primarily controlled by their geographic setting, in particular by their latitude and prevailing climatic conditions (wet/maritime to dry/continental). In general, glaciers are more sensitive to climate

TCD
7, 267–319, 2013

change in maritime regions with high precipitation and mass turnover (Oerlemans, 2001; Hoelzle et al., 2003; De Would and Hock, 2005; Benn and Evans, 2010).

However, local topographic and microclimatic conditions determine the behavior of glaciers at smaller scales (e.g. within a mountain group). Thus, different behavior can be observed among neighbouring glaciers in response to the same climatic forcing (e.g. Kuhn et al., 1985). These differences mainly depend on the geometry of the glaciers (hypsometric distribution of area vs. altitude, size, slope, aspect), but are also related to the physical characteristics of the surrounding terrain, source of nourishment and debris coverage, which control the local energy and mass balance (Furbish and Andrews, 1984; Benn and Lehmkuhl, 2000; Machguth et al., 2006; Chueca et al., 2007). In addition, feedbacks influence the reaction of individual glaciers to the fluctuations of climate. The most important ones are surface albedo and geometric adjustments (e.g. surface lowering and disintegration), which influence radiative and sensible heat fluxes (Paul et al., 2005; Carturan and Seppi, 2007; WGMS, 2009; Paul, 2010; Carturan et al., 2012b).

The highly variable response (i.e. changes in length, area or thickness) complicates the assessment of future glacier behavior under different climate change scenarios. On the other hand, studying the spatial variability of glacier fluctuations and their relationship to climatic changes, can be seen as a good opportunity to improve our knowledge of processes and feedbacks in action. Moreover, it is a valuable tool for the quantification of the current decoupling of glacier geometries from equilibrium conditions under current warming (Zemp, 2006).

The most immediate indication of the degree of equilibrium of glaciers is mass balance. Generally, a few glaciers with suitable characteristics in regard to their size and accessibility are monitored with the “direct” method (Østrem and Brugman, 1991), but their representativeness for entire regions or mountain ranges is often unknown. Hence, the extrapolation of measured mass balances to nearby glaciers is challenging, as local characteristics affect the sensitivity of individual glaciers (Carturan et al., 2009a; Fountain et al., 2009; Kuhn et al., 2009).

TCD
7, 267–319, 2013

Other variables closely related to the mass balance, such as the Equilibrium Line Altitude (ELA) or the Accumulation Area Ratio (AAR, ratio between accumulation area and total area), can be used for assessing the direct impact of climate change (e.g. an upward shift of the ELA) or the degree of imbalance of glaciers with respect to current climate conditions (e.g. the deviation of the AAR from a balanced budget AAR). However, the relationship with mass balance is not univocal, in particular in high-mountain environments where avalanches, debris cover and topographic shading can strongly affect the spatial distribution of the mass balance (Braithwaite, 1984; Kulkarni, 1992; Clark et al., 1994; Benn and Lehmkuhl, 2000; Zemp, 2006; Braithwaite and Raper, 2009).

Measuring mass balance with the geodetic method increases the spatial coverage (Cogley, 2009) and gives the total volume change also considering processes not measured at the surface (e.g. basal melting) and regions that are not measured (e.g. steep parts or zones with seracs). Furthermore, the geodetic method is required to calibrate the field measurements from time to time (e.g. Thibert et al., 2008; Haug et al., 2009; Huss et al., 2009; Zemp et al., 2010) and can be used for assessing the representativeness of the measured glaciers for entire mountain ranges, as well as an analysis of the spatial pattern of glacier thickness changes over large regions (Dyurgerov and Meier, 2005; Haeberli et al., 2007; Paul and Haeberli, 2008). The modern tool for such assessments is the multi-temporal differencing of Digital Terrain Models (DTM), whose generation has recently been improved in terms of accuracy, automation and resolution by airborne laser scanning using LiDAR (Light Detection and Ranging) technology (e.g. Arnold et al., 2006; Geist and Stötter, 2007; Knoll and Kerschner, 2009; Joerg et al., 2012). The dependence of observed fluctuations on local variables (e.g. topographic attributes) can be investigated by means of statistical analyses, in order to assess why different glaciers react in different ways to the same climatic forcing (e.g. Chueca et al., 2007; Abermann et al., 2009, 2011; Vanlooy and Forster, 2011).

Since the 1980s, the European Alps have been experiencing a phase of intense glacier area and volume loss, which was also observable worldwide (UNEP/WGMS,

TCD
7, 267–319, 2013

2008; WGMS, 2008). Regional-scale analyses of this recession period in the Alps were carried out by several authors, who focused mainly on area and length changes using multi-temporal remotely sensed data and existing ground measurement series (e.g. Paul et al., 2004, 2007a; Lambrecht and Kuhn, 2007; Zemp et al., 2008). The spatial variability of glacier elevation changes from DTM differencing was analyzed by fewer studies, mainly in Switzerland (Paul and Haeberli, 2008) and in Austria (Abermann et al., 2009). Regional assessments of glacier area and length changes in the Italian Alps over this period were carried out in the Lombardia region (Citterio et al., 2007; Maragno et al., 2009; Diolaiuti et al., 2011), while in South Tyrol Knoll and Kerschner (2009) also analyzed volume changes.

In this work we used two Landsat scenes and two DTMs acquired in the 1980s and 2000s for quantifying changes in glacier length, area and volume over the entire range of the Ortles-Cevedale group. We examine topographic parameters, their changes through time and their possible role in controlling the spatial variability of changes. We also quantify the current decoupling of glacier geometries from equilibrium conditions by comparing the extent of accumulation areas to their balanced-budget size. This analysis is also aiming at providing an environmental context for the recently undertaken paleo-climatological investigations on Mt. Ortles (Gabrielli et al., 2010, 2012; Gabrieli et al., 2011).

2 Study area and data sets

2.1 Study area

The Ortles-Cevedale group is located in the Eastern Italian Alps and covers an area of 1638 km^2 (Fig. 1). The highest peaks of the mountain group, Mt. Ortles (3905 m), Mt. Gran Zebrù (3851 m) and Mt. Cevedale (3769 m), are aligned in a NW-SE direction. Rather sharp ridges exist in the north-western area, which is composed of sedimentary rocks (dolomites and limestones), while metamorphic rocks (mica schists, paragneiss and phyllites) prevail elsewhere, forming more rounded reliefs. These lithologic differences have an important influence on the terrain morphology and significantly affect the distribution and morphology of the glaciers (Desio, 1967).

The glaciers of the Ortles-Cevedale constitute a major resource for the local population, as they have great touristic appeal and are precious water resources for hydropower generation, potable water supply and agriculture. The group is one of the largest glacierized regions of the southern side of the European Alps (76.8 km^2, about 3.5 % of the total Alpine glacierized area) and hosts the largest Italian valley glacier (Forni, 11.3 km^2). Like in most of the European Alps, the Ortles-Cevedale glaciers have been retreating since the end of the Little Ice Age (LIA), with phases of temporary readvance in the 1890s, 1910–20s and in the 1970–80s. A new phase of strong retreat began in the 1980s, and still continues (Citterio et al., 2007; CGI, 1978–2011, Zemp et al., 2008).

Figure 2 shows the monthly regime of average temperature and precipitation at the Careser dam weather station (2605 m a.s.l.), which is located in the southern part of the study area (Fig. 1). The Ortles-Cevedale group lies in a transition zone between the "inner dry alpine zone" to the north (Frei and Schär, 1998), and the wetter area under the influence of the Mediterranean Sea, to the south. In the valleys, the annual precipitation ranges from ~900 mm at the southern edge of the group to ~500 mm at the northern edge. Precipitation increases with altitude reaching values up to 1300–1500 mm a^{-1} at 3000–3200 m within the glacierized areas of the group (Carturan, 2010; Carturan et al., 2012a). The mean annual 0 °C isotherm is located around 2500 m.

2.2 Data sets

Two early-autumn Landsat scenes (path 193, row 28 from 20 September 1987 and 31 August 2009; downloaded from http://glovis.usgs.gov) were selected, based on the absence of fresh snow and the presence of very low cloud cover. The DTMs were acquired between 1981 and 1984 and between 2005 and 2007, with different methods and spatial resolutions by the local administrations of the Ortles-Cevedale group

(Table 1). Printed aerial photos (black and white, scale 1 : 10 000 to 1 : 20 000, years 1982 and 1983) and digital orthophotos (colors, resolution 0.5 × 0.5 m, years 2006–2008) were also available. From now on we simply refer to the 1980s and 2000s as beginning and end of the investigated period.

Direct mass balance measurements in the Ortles Cevedale group are available for the Careser Glacier since 1967 (Zanon, 1992; Carturan and Seppi, 2007, WGMS, 2011). Other long-term mass balance series in this group exist for the Fontana Bianca Glacier (1984–1988, restarted in 1992) and for the Sforzellina Glacier (since 1987) (CGI, 1978–2011; WGMS, 2008; C. Smiraglia, personal communication, 2012).

A long series (since 1930) of meteorological data at high altitude exist for the Careser dam weather station (2605 m a.s.l.), which provide additional information for interpreting the observed glacier changes. Observations used in this study include daily data of precipitation, 2 m air temperature and snow observations (fresh snow and total snow depth) over the period 1959–2009.

3 Methods

3.1 Calculation of glacier area and length changes

Two glacier inventories, including 165 glacier basins in the Ortles-Cevedale group, were created from the two Landsat images, to calculate area changes from the 1980s to the 2000s. The Landsat scenes were processed using the ESRI ArcGIS software, in the UTM-WGS84 (Universal Transverse Mercator, zone 32, World Geodetic System 1984 datum) coordinate system. A thresholded band ratio image (Landsat visible band TM3 divided by the shortwave infrared band TM5) was used for classifying the debris-free areas of glaciers (e.g. Paul and Kääb, 2005; Andreassen et al., 2008; Paul et al., 2011). Manual post-processing, using contrast-enhanced composites of Landsat scenes (bands TM5, TM4 and TM3 as red, green and blue) and aerial photos, was required to remove inclusion of lakes, and for correcting misclassifications over

TCD
7, 267–319, 2013

shadowed and debris-covered areas. In a few cases a direct inspection in the field was required for assessing the lower boundary of heavily debris-covered glaciers in 2009, while in 1987 the margins were more evident in the imagery, due to lower debris cover as well as more convex and sharp fronts. In many cases frontal moraines visible in the 2000s aerial photos (e.g. Fig. 4) were helpful for correcting the automatic classification of debris-covered fronts in 1987, since these moraines mark the most advanced position of the glaciers during the mid 1980s (CGI, 1978–2011). For the limited areas covered by clouds in the Landsat scenes (less than 1 % of the total glacierized area), we reconstructed the glacier outlines by using aerial photos and the closest in time Landsat image available.

The identification of glacier units was based on former inventories. We mainly used the World Glacier Inventory (WGMS, 1989), adding two small units (Alto del Marlet and Cima della Miniera) that were reported in previous works (CNR-CGI, 1959–1962; Desio, 1967). The outlines of the drainage basins were derived from a flow direction grid calculated from the most recent DTMs, which have a higher spatial resolution (Table 1). The classified grids of two glacierized surface types (debris-free and debris-covered areas), which were obtained from each Landsat scene, were converted to polygon shape-files and then intersected with the shape-file of the digitized drainage basins. Thus, for each drainage basin, the total glacierized area was calculated as the sum of the areas of the two surface types.

The minimum size for an ice body was set to 0.01 km^2 (Paul et al., 2009). Glacierets were distinguished from glaciers based on the absence of evidence of motion and/or lack of a clear distinction between accumulation and ablation areas on aerial photos. Topographic parameters for each ice body were then calculated from the DTMs of the two periods, extracting minimum, maximum and mean values from the grids of elevation, slope, aspect, and clear-sky global radiation in summer (June to September). The average elevation used in the analyses is therefore the "area averaged" elevation of each glacier. Since aspect is a circular parameter, the mean value for each glacier was calculated as the arc tangent from the respective mean values of the sine and cosine

TCD
7, 267–319, 2013

grids of terrain aspect (Manley, 2008; Paul et al., 2009). We made the assumption that the glacier changes which occurred between the acquisition dates of DTMs (Table 1) and the respective Landsat scenes were negligible in comparison to the total changes occurred between the 1980s and the 2000s.

3.2 Calculation of glacier volume changes and average mass budget

Before calculating the elevation changes over glaciers, all the DTMs were resampled to a grid cell size of 20 m (i.e. the maximum cell size of the original DTMs, Table 1). Then they were co-registered and checked for possible elevation- or slope-dependent biases (Berthier et al., 2006; Paul, 2008; Gardelle et al., 2012). The results showed no clear dependencies of the elevation differences between the DTMs and elevation or slope, over stable terrain. Therefore, we did not apply any correction to the elevation difference grid calculated from the co-registered DTMs (see Sect. 4.2 for considerations on the accuracy). The total volume change ΔV (m^3) for each glacier was calculated as follows:

$$\Delta V = \overline{\Delta z} \cdot A_1 \tag{1}$$

where $\overline{\Delta z}$ is the average elevation change between the final DTM_{2000} and the initial DTM_{1980}, over the initial area A_{87}. The area-averaged net geodetic mass budget rate ($m\,w.e.\,a^{-1}$), referred to as "average mass budget" from now on, was then calculated as:

$$b = \frac{\Delta V \cdot \rho}{\bar{A}} \cdot t^{-1} \tag{2}$$

where ρ is the mean density, $\bar{A}$ is the average of the initial (A_{87}) and final (A_{09}) areas, and t is the time interval (yr) between the two periods. We used a mean density of 850 $kg\,m^{-3}$ (rather than 900 $kg\,m^{-3}$), as suggested by the literature for glaciers that are thinning and losing old firn at mid-elevation areas (Krimmel, 1989; Sapiano et al., 1998; Elsberg et al., 2001; Fischer, 2011).

TCD
7, 267–319, 2013

3.3 Extent of accumulation areas and current degree of imbalance

Useful information on the extent of accumulation areas was derived from the two Landsat scenes by assuming that the late-summer snow covered area (SCA) is identical with the accumulation region. We are aware that this is not fully and not always correct, but other studies have shown that it is a reasonable proxy nevertheless (e.g. Rabatel et al., 2008). On both acquisition dates, the snowline was well defined and the SCA was very close to its annual minimum. According to the meteorological observations of the Careser dam personnel, the 1987 scene was acquired at the end of the ablation season, right after a two-week period of warm and dry weather and just prior to the first snow of the following accumulation season on 24 September. The 2009 scene was acquired shortly before the end of the ablation season, as confirmed by our observations on La Mare glacier (that is since 2003 also subject to direct mass balance measurements; Carturan et al., 2009b), where the SCA on 31 August (77 ha), was only 11 % larger than its minimum (69 ha), reached in mid September. The related values for the Accumulation Area Ratio (AAR) are 0.37 and 0.33. The accumulation areas visible in the Landsat scenes are also fairly representative of their long-term extent. In particular, the scene of 2009 shows snow conditions close to the average extent of accumulation areas during the preceding decade (Table 2). In addition, the two series of direct observations available in the Ortles-Cevedale group (Careser and Fontana Bianca glaciers) show that the average AAR in the period between 1987 and 2009 (0.01 and 0.10, respectively) is within the range of the arithmetic mean values of the AAR derived from the two Landsat scenes (0.01 and 0.22, respectively).

The SCA was mapped based on differences in reflectance in the near infrared band of the Landsat scenes (TM4, 0.76–0.90 µm). We applied the procedure described in the technical specifications of GlobGlacier (2008), for converting the digital numbers to at-satellite radiance, and for deriving the Top-Of-Atmosphere Reflectance (TOAR) accounting for the sun-earth distance, the solar constant and the solar zenith angle. Afterwards, a radiometric correction for topographic effects has been applied to the

TOAR, to account for slope and aspect effects on surface irradiance (different contributions of direct and diffuse irradiance). We tested the Minnaert and Ekstrand correction methods for this (Minnaert, 1941; Ekstrand, 1996), which are both suitable for steep alpine terrain (Law and Nichol, 2004; Törmä and Härmä, 2003; Ekstrand, 1996). In comparison with false-color composites the Ekstrand method provided the best results and was selected for the corrections.

The maps of corrected TOAR were analyzed to determine a threshold for separating snow-covered and snow-free areas. This was rather easy as snow showed a very different reflectance compared to ice, in both scenes (see Fig. 5). In 2009 field data were available to check the thresholds, while in 1987 there were no direct observations and we adjusted the thresholds by comparing automatic classifications with a contrast-enhanced false-color composite image (using TM bands 4, 3 and 2 as RGB in sunlight and bands 3, 2 and 1 in shadow).

The SCA and the snowline altitude (SA) from the 1987 and the 2009 images were examined for eight aspect classes. The SA position was determined by intersecting the lower limit of the SCA with the DTMs (McFadden et al., 2011). Avalanche-fed glaciers were not considered in SA calculations, as avalanches may significantly lower it locally.

An assessment was made of the degree of imbalance of existing glaciers with respect to the current extent of the accumulation areas, derived from the 2009 Landsat scene. As mentioned above and shown in Table 2, the SCA and SA derived from this scene (SCA_{09} and SA_{09}) provide a quite good representation of the average extent of accumulation areas and position of the ELA in the last decade. Therefore, we compared the AAR_{09} ($= SCA_{09}/A_{09}$) and the ELA_{09} ($= SA_{09}$) to theoretical "balanced-budget" conditions. Field evidence from glaciers subjected to direct mass balance measurements in the Ortles-Cevedale group indicates an average value of 0.5 for the balanced-budget AAR0 (CGI, 1978–2011; WGMS, 2008, 2011). The fractional change of the total area (p_s) necessary to reach equilibrium was calculated by comparing the AAR_0 with the AAR_{09}, as follows (Bahr et al., 2009):

$$p_s = \alpha_r - 1 \tag{3}$$

where α_r is the ratio AAR_{09}/AAR_0, which provides a measure of the extent to which each glacier is out of equilibrium (Dyurgerov et al., 2009). For the glacierets, where there is no transfer of mass from an accumulation to an ablation area, we adopted an AAR_0 value of 1.

3.4 Analysis of controls

To highlight the controlling factors of the current glacier shrinkage, the area and elevation changes of the Ortles-Cevedale glaciers were analyzed in two steps, examining (i) the entire Ortles-Cevedale glacier system and (ii) the individual responses of individual glaciers. For (i) we investigated the relative change in the frequency distribution of glacierized areas, and the elevation changes, for classes of elevation, slope, aspect and summer clear-sky radiation. Then a correlation analysis was performed considering a sample of 112 ice bodies (those which survived in 2009). The 10 variables used in the statistical analysis were the average (1980s to 2000s) values of: mass budget, elevation, elevation range, slope, aspect, summer clear-sky radiation, AAR, fractional debris cover, area, and the "avalanche ratio" (Av) calculated as follows (Hughes, 2008):

$$Av = \frac{A_{av}}{A} \tag{4}$$

where A_{av} is the avalanche contributing area, computed from a flow direction grid and from a slope grid (both derived from the DTM), and A is the total area of a glacier. The aspect was indexed before calculations, by assigning the value 9 to south, 7 to south-west and south-east, 5 to east and west, 3 to north-west and north-east, and 1 to north.

TCD
7, 267–319, 2013

4 Accuracy assessment

4.1 Area and snow cover changes

For debris-free glaciers, the typical accuracy of automatic mapping from Landsat TM scenes is about 2–3 %, as reported by earlier assessments based on comparisons with manual delineations on higher-resolution images (e.g. Paul et al., 2002; Andreassen et al., 2008). A test carried out for a subset of 15 debris-free glaciers on Ortles-Cevedale confirmed this accuracy, revealing small (2–4 %) discrepancies mainly due to marginal debris-covered areas (i.e. medial moraines and/or margins of the ablation area). A greater uncertainty (one order of magnitude larger) affects the mapping of larger debris-covered areas, which have to be manually corrected. Figure 4 clearly shows the difference between the Landsat TM automatic mapping and the post-processed delineation on a heavily debris-covered glacier. The accuracy of this post-processing procedure, which was mainly carried out on aerial photos, depends on: (i) characteristics of debris-covered areas (e.g. optical contrast to the surrounding terrain, occurrence of features indicating buried ice), (ii) characteristics of the images (contrast), and (iii) analyst experience. In the absence of reference data, one possibility to estimate the precision of the derived glacier areas comes from an independent multiple digitization of the same set of glaciers. This procedure was carried out for five debris-covered glaciers of the Ortles-Cevedale, of different sizes, resulting in a standard deviation of 3 %, which confirms previous tests on glaciers with similar characteristics (Paul et al., 2012; Rastner et al., 2012).

The accuracy of the automatic mapping of SCA from the Landsat scenes was assessed by comparing the results of the automatic procedure with a snow cover map that was drawn from field surveys carried out on Careser and La Mare glaciers on 13 September 2009 (Fig. 5). The automatic mapping provided a 11 % larger SCA than directly surveyed on the ground. Part of this discrepancy can be attributed to shortcomings in the classification method (e.g. in deep shadows), but as observed on La

TCD
7, 267–319, 2013

Mare glacier (Sect. 3.3) the largest part has to be attributed to an actual reduction of the SCA from 31 August to 13 September.

4.2 Elevation changes and mass budget

The accuracy of the derived elevation and volume changes from the geodetic method depends mainly on the accuracy of the used DTMs. When the mean volume change rates are compared to the mean net budget rate as measured in the field, differences due to the unknown density and basal melting or collapse occur. So a direct comparison of both values is challenging (e.g. Fischer, 2011). Uncertainties related to the DTMs depend primarily on the acquisition technique of the elevation data (e.g. optical, LiDAR, radar), on the procedure used for their extraction from raw data, and finally on their processing prior to differencing (e.g. co-registration and resampling). Recent works report the existence of elevation and slope-dependent biases when DTMs of different resolution are compared (Berthier et al., 2006; Paul, 2008; Gardelle et al., 2012), suggesting the implementation of a correction procedure based on the maximum curvature (Gardelle et al., 2012). However, we did not find such a dependency in our co-registered DTMs and have thus not applied a correction (Sect. 3.2). A possible explanation might be that these slope-dependent errors mainly arise when downscaling lower resolution DTMs to higher resolution, while in the present work original DTMs with 2 to 10 m resolution we upscaled to a grid cell size of 20 m (i.e. the maximum cell size of the original DTMs, Table 1).

The accuracy of the DTM differencing was assessed by applying the geostatistical procedure described in Rolstad et al. (2009). They mention that uncertainties depend on the standard error of individual grid point elevation differences between the two DTMs, as well as on the size of the averaging area (i.e. the size of the ice body) and on the scale of the spatial autocorrelation of elevation differences. The geostatistical procedure takes into account the spatial correlation of the elevation differences, quantified over "training areas" on stable bedrock. According to this procedure, DTM differencing leads to a propagated uncertainty in area-averaged net geodetic mass budget rates ranging from ±0.03 to ±0.26 m w.e. a^{-1}, averaging to ±0.08 m w.e. a^{-1} for glaciers with average area of 0.79 km^2 in the Ortles-Cevedale group.

Density assumptions may also introduce uncertainties, in particular during periods with changes in the density of the firn layer (Haug et al., 2009). Such changes likely also occurred in the Ortles-Cevedale, because the DTMs used in the calculations were acquired in the first half of the 1980s (Table 1), when glaciers still retained firn layers accumulated in the 1960s and 1970s. For this reason a mean density of 850 kg m^{-3} was used. Error estimates provided by the literature indicate an uncertainty of ∼ 6 % in these cases (Sapiano et al., 1998, Elsberg et al., 2001).

5 Results

5.1 Area and length changes

The Ortles-Cevedale mountain group was subdivided into 165 glacier basins. While small glaciers and glacierets prevail in number (with only two glaciers exceeding 5 km^2) much of the glacierized area is concentrated in mountain and valley glaciers ranging from 1 to 5 km^2 (Fig. 6). We note that 32 ice bodies were already extinct in the 1980s, and 21 glacierets completely disappeared from the 1980s to the 2000s. Over the same period 14 mountain glaciers transformed into glacierets. All 14 valley glaciers kept their shape, but some of them are about to lose their valley tongue and will soon transform into mountain glaciers. Table 3 shows the detected changes of key parameters for the entire glacier system (i.e. all the ice bodies are taken as one large glacier) and for the subset of the 112 ice bodies existing in 2009. Since 1987, 23.4 % of the initial glacierized area (100.3 km^2) has been lost and the debris covered area increased by 19 %. In 2009, 41 ice bodies were "debris-covered", 18 more than in 1987. About 90 % of these 41 glaciers can be characterized as "avalanche-fed".

The average elevation of the glacierized area did not increase significantly (3110 m in the 1980s, 3124 m in the 2000s). Individual glacier units displayed contrasting behavior, with some glacierets and small glaciers showing a significant increase in mean elevation, due to the complete loss of their lower parts or sub-units. In contrast, the largest decrease of average altitude was observed where steep glacierized slopes located at the top of accumulation areas ablated completely (e.g. Solda glacier). The elevation range (difference between maximum and minimum elevations) exhibited a significant and widespread decrease (−74 m). This reduction was mainly caused by an upward shift of the minimum elevations (+53 m on average), and secondarily by the downward change of maximum elevations (−27 m on average).

Negligible changes were observed for the mean slope of the glacierized areas, in particular for the largest glaciers, while the smaller ice bodies displayed more variability. Increasing slopes were found over small residual patches in shadowed areas, with avalanched snow now accumulating at their base, while decreasing slopes were observed in the case of deglaciating cliffs and couloirs. Although generally small (−3 % on average) a general tendency toward a reduction of clear-sky radiation during summer was recognized, originating from a more efficient shadowing of rock walls over the lowering and retreating ice surfaces, which mainly have a northern exposure, as explained below.

The reduction of the glacier areas from the 1980s to 2000s can be observed in Fig. 1, where the glacierized areas in the two epochs are overlapped. The change in area since the 1980s is around −20 % for most glaciers larger than 1 km^2 (Fig. 7a, Table 4), with the exception of Careser Glacier, which lost 48 % of its initial area. The scatter in areal reductions increases strongly for glaciers smaller than 0.5 km^2 and a tendency towards a greater relative area loss with decreasing initial size is also observable. The terminus retreats were proportional to the initial length ($R = 0.70$), with valley (longer) glaciers retreating more than mountain (shorter) glaciers (Fig. 7b). Cumulated values of retreat peak at −610 m for Forni and Forcola glaciers (−27.7 $m\,a^{-1}$). In some cases, single glaciers broke up into smaller ice bodies and length changes could not be measured. The most striking example is the Careser Glacier, where the

TCD
7, 267–319, 2013

widespread emergence of the bedrock led to the fragmentation of the parent glacier (Fig. 1).

In Fig. 8 we show the change in the frequency distribution of glacierized areas for classes of elevation, slope, aspect and summer clear-sky radiation. The area covered by glaciers decreased at all elevations. Figure 8b suggests an increase of the relative area losses towards the steeper regions, which usually accumulate less snow and normally have a lower ice thickness. Most of the glaciers lie on northern slopes, and the relative area change was higher over southern exposures (Fig. 8c). Nevertheless, strong area losses were also found in shaded regions (Fig. 8d; e.g. on the formerly fully glacierized north cliffs at the top of Solda Glacier).

5.2 Elevation changes and mass budget

Large elevation changes occurred in the Ortles-Cevedale glacier system (Fig. 9). The total volume change has been $-1.58\,\mathrm{km}^3$. Surface lowering prevailed at all elevations, with the exception of the Mt. Ortles summit area (Alto dell'Ortles Glacier), above 3800 m a.s.l., where negligible changes have been detected. The average lowering rate was $0.71\,\mathrm{m\,a^{-1}}$, with maximum rates of 3.5–4 $\mathrm{m\,a^{-1}}$ in the lower parts of four valley glaciers (Forni, Basso dell'Ortles, Lunga and La Mare). Many episodes of collapsing subglacial cavities were observed in the field, which tend to accelerate the fragmentation of low-altitude, stagnant portions of glaciers. The glaciers which still retained some snow cover at the end of the ablation period have much smaller lowering rates (from 0 to $0.5\,\mathrm{m\,a^{-1}}$) in their upper parts. In contrast, glaciers with small or no snow covered areas show high lowering rates over the entire surface, e.g. Lasa Glacier (from 0.5 to $1.0\,\mathrm{m\,a^{-1}}$) and, in particular, Careser Glacier (from 1.0 to $2.5\,\mathrm{m\,a^{-1}}$).

Notably, the average mass budget was negative for all the ice bodies in the Ortles-Cevedale group. The mean of the 112 individual mass budgets is $-0.69\,\mathrm{m\,w.e.\,a^{-1}}$, while the area-weighted mean is $-0.68\,\mathrm{m\,w.e.\,a^{-1}}$. The individual values are distributed normally and show less dispersion for the glaciers than for the glacierets (standard deviations are 0.17 and $0.35\,\mathrm{m\,w.e.\,a^{-1}}$, respectively). The mean mass budgets for the glacierets and glaciers are substantially identical ($-0.68\,\mathrm{m\,w.e.\,a^{-1}}$ and $-0.70\,\mathrm{m\,w.e.\,a^{-1}}$, respectively). The spatial variability of the geodetic mass budget is relatively low, with a few exceptions (Fig. 10). The two extremes among all the glaciers of the Ortles Cevedale group are the Alto dell'Ortles ($-0.18\,\mathrm{m\,w.e.\,a^{-1}}$) and Careser ($-1.43\,\mathrm{m\,w.e.\,a^{-1}}$). The scatterplot in Fig. 10 shows no clear relationship between the mass budget and the initial glacier size, as found in the studies by Paul and Haeberli (2008) and Paul (2010), but as was observed for area changes, the scatter increases among smaller ice bodies. For glaciers larger than $0.7\,\mathrm{km^2}$ the mass budget ranged from 0.40 to $0.80\,\mathrm{m\,w.e.\,a^{-1}}$, with the exception of the above-mentioned Careser Glacier.

The vertical profile of the elevation changes over the entire glacierized area (Fig. 11a) shows maximum lowering rates ($-1.3\,\mathrm{m\,a^{-1}}$) at $\sim 2700\,\mathrm{m\,a.s.l.}$ Interestingly, below this altitude, decreasing lowering rates were found (minimum of $-0.2\,\mathrm{m\,a^{-1}}$ at $2300\,\mathrm{m\,a.s.l.}$), maybe as a result of the large share of debris-covered glaciers. Flat areas lowered more rapidly than steeper areas (Fig. 11b), and stronger elevation losses were detected over slopes with higher radiation inputs (Fig. 11c, d).

5.3 Extent of snow covered area and current degree of imbalance

The Snow Covered Area (SCA) was $7\,\mathrm{km^2}$ (23.4 %) smaller in 2009 than in 1987 (Fig. 12). The average snowline altitude ($\overline{\mathrm{SA}} = (\mathrm{SA}_{87} + \mathrm{SA}_{09})/2$) ranged from 3094 m on northern slopes to 3335 m on southern slopes. $\overline{\mathrm{SA}}$ was 45 m higher on areas exposed to the east (3223 m), than to the west (3178 m). The average SA of the glacier system, normalized as a function of the exposure, was at 3215 m in 1987 and 3223 m in 2009, showing negligible differences.

The index α_r ($\mathrm{AAR}_{09}/\mathrm{AAR}_0$ in Eq. 3) is at present lower than 1 in all cases except two (Pracupola and Alto dell'Angelo), indicating that nearly all the glaciers are still too large and have to reduce their area (by 41 % on average) in order to reach balanced budget under the current climatic conditions. For 25 (21 glacierets and 4 glaciers) out of 112 cases, the resulting equilibrium areas are less than 1 ha, thus indicating impending extinction. Among the glaciers larger than 1 km^2, further remarkable area losses are expected for Careser (−87 %) and Lasa (−66 %) glaciers. Conditions closer to equilibrium were found for the highest altitude glacier (Alto dell'Ortles, mean elevation 3425 m). Large area losses are expected in general for valley glaciers (−34 % on average). Among them, Cevedale and Dosegù glaciers still have a relatively large accumulation area (AAR_{09} = 0.45) and are closer to equilibrium.

5.4 Analysis of controls

The results of the correlation analysis among average geodetic mass budgets and nine other variables is shown in Table 5. The subset of 79 glaciers showed highly significant (0.01 level) correlation of mass budget with slope, AAR and elevation range. The correlation with elevation and avalanche ratio is less significant (0.05 and 0.10 level, respectively), while there is an absence of significant correlation of the mass budget with aspect, clear-sky radiation, debris cover and area. The glaciers with higher elevation range and higher mean elevation also have a higher AAR. The AAR is in turn highly correlated with area and (inversely) with the debris cover. The glaciers which have higher radiation inputs (i.e. with less topographic shading) are located at higher altitudes, and vice versa. On the other hand, increasing debris cover enables the existence of ice masses at lower elevations, and is generally related to the avalanche activity on small glaciers.

The group of 33 glacierets produced quite different results. Among the analyzed variables, the debris cover and the avalanche ratio displayed the highest correlation with mass budget, followed by slope and, with a lower significance, by area. The absence of a significant correlation with elevation and with AAR (in contrast to results provided by glaciers) is remarkable but somewhat expected for glacierets. The glacierets with higher altitude have less debris cover and are less shielded from solar radiation. Slope is inversely correlated with aspect and clear-sky radiation, while it is directly correlated

TCD
7, 267–319, 2013

with debris cover and elevation range. As was observed for glaciers, the ice bodies which have higher debris cover are also mainly avalanche-fed.

6 Discussion

6.1 Glacier changes and controls

The area loss rate of the Ortles-Cevedale glacier system was $-1.1\,\%\,a^{-1}$ (referred to the initial area in 1987). This value is about half that of other recent alpine-wide estimates ($-2\,\%\,a^{-1}$ from 1984 to 2003, Paul et al., 2011), but it is similar to results of previous investigations in the European Alps. Paul et al. (2004), found an area loss rate of $-1.3\,\%\,a^{-1}$ for the Swiss glaciers from 1985 to 1999, while Lambrecht and Kuhn (2007) calculated a rate of $-0.6\,\%\,a^{-1}$ for the Austrian glaciers during the period 1969–1998. However, the latter includes the expansion period of 1973–1985. If total area change in this period is assumed to be close zero, the rate over the 1985–1998 period is $-1.2\,\%\,a^{-1}$. Abermann et al. (2009), calculated an increase in area loss rates from $-0.4\,\%\,a^{-1}$ in the period 1969–1997 to $-0.9\,\%\,a^{-1}$ in the period 1997–2006 in the Austrian Ötztal Alps. Concerning the Italian Alps, Knoll and Kerschner (2009) quantified a reduction rate of $-1.4\,\%\,a^{-1}$ for the South Tyrol glaciers from 1983 to 2006, highlighting a significantly lower reduction rate ($-1.1\,\%\,a^{-1}$) for the portion of the Ortles-Cevedale glaciers that lies in the province of Bolzano, which is consistent with our results in this area ($-1.0\,\%\,a^{-1}$). Larger reduction rates ($-1.8\,\%\,a^{-1}$) were found from 1981 to 2003 for the glacier system of the Dosdè-Piazzi group, about 20 km west of Ortles-Cevedale (Diolaiuti et al., 2011). Citterio et al. (2007), calculated an area reduction of $-1.5\,\%\,a^{-1}$ for 249 glaciers in the Lombardia region from 1992 to 1999. Finally, Maragno et al. (2009), estimated $-0.9\,\%\,a^{-1}$ for the Adamello group (35 km south-west of Ortles-Cevedale) during the period 1983–2003.

The spatial pattern of the area changes shows significant area losses even at high altitudes (Fig. 8a), causing a substantial lack of adjustment of the average elevation of the glacier system (+14 m). This can be explained by considering the physical characteristics of the high-altitude glacierized areas of the Ortles-Cevedale group, which are typically steep and convex and receive relatively little snow accumulation during winter. These high elevation areas should benefit from the accumulation of wet snow during the warmer part of the year. However, due to less abundant summer snow falls (Fig. 13c), they are often exposed to net ablation during the summer.

Factors causing negative feedbacks on glacier wastage were detected, such as the increase in debris cover and the decrease of clear-sky radiation during summer (due to increased topographic shading for some glaciers). Overall, these feedbacks were not effective so far in offsetting the effects from increasing temperatures (Fig. 13a).

The average geodetic mass budget of the glaciers is indeed highly negative ($-0.7\,\mathrm{m\,w.e.\,a^{-1}}$) and close to the average of nine glaciers with long-term direct measurements from the European Alps ($-0.8\,\mathrm{m\,w.e.\,a^{-1}}$) during the same period (Zemp et al., 2005; WGMS, 2008, 2009 and 2011). However, these two estimates come from different methods, which can give quite different results depending e.g. on density assumptions, basal or internal melt, and errors in measuring and/or extrapolating direct measurements (Krimmel, 1999; Fischer, 2011). On the other hand, the two methods provided very similar results on Careser Glacier from 1983 to 2006 ($-1.43\,\mathrm{m\,w.e.\,a^{-1}}$ (geodetic) and $-1.39\,\mathrm{m\,w.e.\,a^{-1}}$ (direct)). Similarly, good results were obtained also for the other two glaciers with long-term direct measurements, even if these lack some years (Sforzellina, $-0.86\,\mathrm{m\,w.e.\,a^{-1}}$ (geodetic) and $-1.08\,\mathrm{m\,w.e.\,a^{-1}}$ (direct), the latter missing 6 yr out of 26; Fontana Bianca, $-0.90\,\mathrm{m\,w.e.\,a^{-1}}$ (geodetic) and $-0.86\,\mathrm{m\,w.e.\,a^{-1}}$ (direct), the latter missing 3 yr out of 21).

The elevation changes vs. altitude plot (Fig. 11a) displays a trend that is quite different e.g. from the findings of Lambrecht and Kuhn (2007). In this latter case the trend resembled the vertical balance profile on a "clean glacier" (i.e. a glacier without debris cover), with increasing elevation losses toward the lower areas. In the Ortles-Cevedale group the trend more closely recalls the vertical profile of the mass balance from debris-covered glaciers (e.g. Benn and Lehmkuhl, 2000), with decreasing elevation losses below 2700 m. Actually, the only areas which extend below this altitude in the Ortles-Cevedale are glacier snouts with thick debris mantles (which insulate them, thus reducing ablation), mainly clustered in the area of Mt. Ortles (Solda, Marlet and Finimondo glaciers).

The positive correlation of the average mass budgets of the 79 glaciers with their elevation range, AAR, mean elevation and slope confirms the already mentioned role of the hypsometry in controlling the sensitivity of the glaciers and response to climate fluctuations (Furbish and Andrews, 1984; Benn and Evans, 2010). The negative correlation which was reported by other authors (e.g. Chueca et al., 2007; Paul and Haeberli, 2008) between mass budget and area and between mass budget and potential radiation in summer was not found in the Ortles-Cevedale, probably due to the peculiar characteristics of the Ortles-Cevedale glaciers. Glacier area is indeed highly correlated with the elevation range (i.e. larger glaciers extend farther in altitude and still retain accumulation areas), and the valley tongues of larger glaciers (which should undergo larger mass losses) are already reduced (e.g. Forni Glacier) or are debris-covered (e.g. Solda Glacier). The lack of a correlation between the mass budget and potential radiation might be attributed to the high mean elevation of the glaciers which receive higher radiation inputs (elevation is highly correlated with potential radiation).

A clear difference exists between glaciers which maintain accumulation areas and show dynamic retreat, and glaciers with low elevation ranges, which are almost entirely below the ELA and show down-wasting. The Careser Glacier, whose area and mass loss rates were much higher than average (Figs. 7a and 10), emphasizes the behavior of the latter group. This comparatively flat glacier lies below the ELA and lacked an accumulation area in most of the past 30 yr. It thus behaved like a stagnant block of ice that simply melts down. The lowering of the albedo and increased thermal emission from the growing patches of ice-free terrain likely act as positive feedbacks, i.e. its behavior might already be decoupled from climate change. The continuation of its long-term mass balance series is at risk and care should be taken for interpreting and extrapolating mass balance results on this glacier.

Glacierets and small glaciers displayed a larger variability in the individual response and a less obvious control of their behavior. Notably, elevation and AAR do not correlate with the mass budget, likely because these small ice bodies are more influenced by local topo-climatic conditions, and are somewhat decoupled from regional-scale climatic trends (Kuhn, 1995; Hughes, 2008; DeBeer and Sharp, 2009; Carturan et al., 2012c). Most of them are remnants of formerly much larger glaciers, that are now protected from ablation by topographic shading and/or debris cover, and take advantage of additional snow accumulation by avalanches. Some of them, located in steep terrain at high altitudes, show little change and might in part be composed of cold ice.

6.2 Extent of accumulation area and current degree of imbalance

The comparison of the current values of AAR (AAR_{09}, which fairly reflects the average climatic conditions in the previous decade, Table 2), and the balanced-budged AAR_0 (0.5 for the Ortles-Cevedale) demonstrates that the glaciers of this mountain group will continue to shrink and retreat, even under unchanged climatic conditions. The expected reduction (41 % on average) rises to 53 % if we take into account the small overestimation of the mean AAR in the last 10 yr by using the SCA_{09} (area-weighted mean difference of 0.06 in Table 2).

Interestingly, some glaciers show an apparent discrepancy between their observed slightly negative mass budget and the degree of imbalance which they should experience, given their current low AAR (e.g. Finimondo and Marlet glaciers). This can be explained by considering that in high-mountain environments the spatial distribution of the mass balance and, as a consequence, the value of the AAR_0 can be profoundly affected by avalanching, debris cover, and topographic effects (Benn and Lehmkuhl, 2000; Benn and Evans, 2010). In particular, glaciers with thick and extensive debris cover tend to have much lower values of AAR_0, since ablation rates are lower on these glaciers compared to "clean" ones, largely due to the insulating effect of debris (Nicholson and Benn, 2006).

TCD
7, 267–319, 2013

The balanced-budget ELA (ELA_0), corresponding to the balanced-budget AAR_0 (0.5), was calculated from the hypsometry of all glaciers of the Ortles-Cevedale group and was compared to current observations of the snowline altitude (SA). The SA_{09} (3223 m) is 92 m higher than the current ELA_0 (3131 m) and 156 m higher than the ELA_0 in the 1980s (3067 m). Since however most glaciers were expanding in the first half of the 1980s, a somewhat lower ELA should have been present in the 10–20 preceding years (1960s–1970s). Based on the mass balance series of Careser Glacier we can estimate a mean ELA of 2984 m in the period 1967–1980, which is 239 m lower than the SA_{09} and 83 m lower than the ELA_0 in the 1980s.

The recent behavior of glaciers in the European Alps was characterized by two contrasting periods: 1960s to 1970s leading to a general expansion, and 1980s to 2000s causing a strong recession (Patzelt, 1985; Citterio et al., 2007; Carturan and Seppi, 2007; Zemp et al., 2008). These two periods are clearly recognizable from the meteorological data series recorded at 2605 m by the Careser dam weather station (Fig. 13), which shows strong positive trends for both annual (+0.5 °C per decade) and summer (+0.6 °C per decade) temperatures. From the first to the second period the mean annual temperature increased by 1.6 °C, resulting in an ELA change of 147 m $^{\circ}C^{-1}$. This value lies in the range of 100–170 m $^{\circ}C^{-1}$ reported for alpine glaciers by recent literature (e.g. Brock et al., 2000; Klok and Oerlemans, 2002; Gerbaux et al., 2005; Paul et al., 2007b; Zemp et al., 2007). Although the temperature increase is the dominant characteristic of the observed climate change, the precipitation trends were not favorable as well for the Ortles-Cevedale glaciers, showing a decrease of 2.5 % per decade for both annual and winter values. Solid precipitation exhibited remarkably larger trends (−7.1 %, −4.6 % and −19 % per decade for annual, winter and summer values).

7 Conclusions

In this work we analyzed the changes in area, length and volume of the glaciers in the Ortles-Cevedale group from the 1980s to the 2000s, using two Landsat scenes (from

1987 and 2009) and calculating the difference between two Digital Terrain Models. We also investigated the role of several parameters in controlling the spatial variability of the glacier shrinkage and the degree of imbalance of glaciers by comparing the AAR derived from their end of summer Snow Covered Area (SCA) with the balanced-budget AAR_0.

In the investigated period, the glaciers lost 23 % of their area, displaying no significant adjustments of their mean altitude. In total, 21 ice bodies became extinct and 14 glaciers transformed into glacierets. Average area loss rates ($-1.1\,\%\,a^{-1}$) and mass loss rates ($-0.7\,m\,w.e.\,a^{-1}$) are slightly lower than previously assessed for other regions in the European Alps. In agreement with previous works, the fractional area change of the Ortles-Cevedale glaciers was inversely related to the initial glacier size, while the snout retreat was proportional to the initial length. On the other hand, individual mass loss rates were not related to the initial glacier size and potential radiation, as found in other studies.

The response of the Ortles-Cevedale glaciers is mainly controlled by their hypsometry (slope, elevation and elevation range). Glaciers with large vertical extent still retain accumulation areas and show active retreat, while flat glaciers below the current ELA experienced strong mass losses over their entire surface, reinforced by positive feedbacks like albedo and thermal emission from the increasingly large rock outcrops. Careser Glacier is the most striking example of this behavior, showing mass loss rates which are nearly double the average. In consequence, this glacier which has a 45-yr-long mass balance series, could be lost for measurements very soon. Very small glaciers and glacierets displayed much more variability in their individual response, since they are increasingly influenced by local topo-climatic conditions and somewhat decoupled from regional climate. Among these, those which are avalanche-fed and debris-covered experienced lower mass losses.

To reach equilibrium under the current climatic conditions (last decade), the Ortles-Cevedale glacier system will need to lose ~50 % of its present area. The snowline altitude (SA) is now ~100 m higher than it should be for balanced-budget conditions, given the current hypsometry of all glaciers, and ~250 m higher than it was in the period of short expansion which occurred in the 1960s-1970s. However, peculiar characteristics of individual glaciers in steep areas of the Ortles-Cevedale, leading to the combination of avalanching, increasing debris cover and topographic shading, favour the persistence of somewhat larger glacierized areas in some cases.

Acknowledgements. This work is dedicated to the memory of Roberto Filippi.

This is contribution No 4 to the Ortles Project (www.Ortles.org). The study was funded by the PRIN 2008 Project "The cryosphere degradation in the Central-Eastern Alps. Study of the ongoing changes by analyzing sample areas and key morphological units" (local head A. Carton). Analysis resources were provided by the Interdepartmental Research Center for Cartography, Photogrammetry, Remote Sensing and GIS (CIRGEO), at the University of Padova. We thank the Fondazione Caritro that supported with a grant the visiting scholarship of Roberto Filippi at the Byrd Polar Research Center and EURAC, and Michele Lanzinger (Museo delle Scienze di Trento) for facilitating this visiting scholarship. Topographic data were provided by the Regione Lombardia and by the Autonomous Provinces of Trento and Bolzano. Meteorological data for Careser dam were provided by Meteotrentino. The field work for mass balance measurements on Fontana Bianca Glacier was carried out by the Ufficio Idrografico of the Autonomous Province of Bolzano. The field work for mass balance measurements on Careser Glacier was carried out under the auspices of the Comitato Glaciologico Italiano, in cooperation with Meteotrentino, Museo delle Scienze di Trento, Comitato Glaciologico Trentino – SAT, Dipartimento di Ingegneria dell'Università di Trento. Claudio Smiraglia kindly provided unpublished mass balance data for the Sforzellina Glacier. The comments of Henry Brecher helped to substantially improve the manuscript. Frank Paul acknowledges financial support from the ESA project Glaciers_cci (4000101778/10/I-AM).

References

Abermann, J., Lambrecht, A., Fischer, A., and Kuhn, M.: Quantifying changes and trends in glacier area and volume in the Austrian Ötztal Alps (1969–1997–2006), The Cryosphere, 3, 205–215, doi:10.5194/tc-3-205-2009, 2009.

Abermann, J., Kuhn, M., and Fischer, A.: Climatic controls of glacier distribution and changes in Austria, Ann. Glaciol, 52/59, 83–90, 2011.
Andreassen, L. M., Paul, F., Kääb, A., and Hausberg, J. E.: Landsat-derived glacier inventory for Jotunheimen, Norway, and deduced glacier changes since the 1930s, The Cryosphere, 2, 131–145, doi:10.5194/tc-2-131-2008, 2008.
Arnold, N. S., Rees, W. G., Devereux, B. J., and Amable, G. S.: Evaluating the potential of high-resolution airborne LiDAR data in glaciology, Int. J. Remote Sens., 27, 1233–1251, 2006.
Bahr, D. B., Dyurgerov, M., and Meier, M. F.: Sea-level rise from glaciers and ice caps: a lower bound, Geophys. Res. Lett., 36, L03501, doi:10.1029/2008GL036309, 2009.
Benn, D. I. and Lehmkuhl, F.: Mass balance and equilibrium-line altitudes of glaciers in high mountain environments, Quaternary Int., 65/66, 15–29, 2000.
Benn, D. I. and Evans, D. J. A.: Glaciers and Glaciation, Hodder Education, London, 802 pp., 2010.
Berthier, E., Arnaud, Y., Vincent, C., and Rémy, F.: Biases of SRTM in high-mountain areas: implications for the monitoring of glacier volume changes, Geophys. Res. Lett., 33, L08502, doi:10.1029/2006GL025862, 2006.
Braithwaite, R. J.: Can the mass balance of a glacier be estimated from its equilibrium-line altitude?, J. Glaciol., 30, 364–368, 1984.
Braithwaite, R. J. and Raper, S. C. B.: Estimating equilibrium-line altitude (ELA) from glacier inventory data, Ann. Glaciol., 50–53, 127–132, 2009.
Brock, B. W., Willis, I. C., Sharp, M. J., and Arnold, N. S.: Modelling seasonal and spatial variations in the surface energy balance of Haut Glacier d'Arolla, Switzerland, Ann. Glaciol., 31, 53–62, 2000.
Carturan, L.: Climate Change Effects on the Cryosphere and Hydrology of a High-Altitude Watershed, Ph.D. thesis, TeSAF – University of Padova, 187 pp., 2010.
Carturan, L. and Seppi, R.: Recent mass balance results and morphological evolution of Careser glacier (Central Alps), Geogr. Fis. Din. Quat., 30, 33–42, 2007.
Carturan, L., Cazorzi, F., and Dalla Fontana, G.: Enhanced estimation of glacier mass balance in unsampled areas by means of topographic data, Ann. Glaciol., 50, 37–46, 2009a.
Carturan, L., Dalla Fontana, G., and Cazorzi, F.: The Mass Balance of La Mare Glacier (Ortles-Cevedale, Italian Alps) from 2003 to 2008, Epitome, Proceedings of Geoitalia 2009 congress, Vol. 3, 298, 2009b.

Carturan, L., Dalla Fontana, G., and Borga, M.: Estimation of winter precipitation in a high-altitude catchment of the Eastern Italian Alps: validation by means of glacier mass balance observations, Geogr. Fis. Din. Quat., 35, 37–48, 2012a.
Carturan, L., Cazorzi, F., and Dalla Fontana, G.: Distributed mass-balance modelling on two neighbouring glaciers in Ortles-Cevedale, Italy, from 2004 to 2009, J. Glaciol., 58, 467–486, 2012b.
Carturan, L., Baldassi, G. A., Bondesan, A., Calligaro, S., Carton, A., Cazorzi, F., Dalla Fontana, G., Francese, R., Guarnieri, A., Milan, N., Moro, D., and Tarolli, P.: Current behavior and climatic sensitivity of the lowermost Italian glacier (Montasio Occidentale, Julian Alps), Geogr. Ann. A, in press, 2012c.
CGI (Comitato Glaciologico Italiano): Reports of the glaciological surveys, Geogr. Fis. Din. Quat., 1–34, 1978–2011.
Chueca, J., Julián, A., and López-Moreno, J. I.: Recent evolution (1981–2005) of the Maladeta glaciers, Pyrenees, Spain: extent and volume losses and their relation with climatic and topographic factors, J. Glaciol., 53, 547–557, 2007.
Citterio, M., Diolaiuti, G., Smiraglia, C., D'Agata, C., Carnielli, T., Stella, G., and Siletto, G. B.: The fluctuations of Italian glaciers during the last century: a contribution to knowledge about Alpine glacier changes, Geogr. Ann., 89, A3, 164–182, 2007.
Clark, D. H., Clark, M. M., and Gillespie, A. R.: Debris-covered glaciers in the Sierra Nevada, California, and their implications for snowline reconstructions, Quat. Res., 41, 139–153, 1994.
CNR-CGI (Consiglio Nazionale delle Ricerche – Comitato Glaciologico Italiano): Catasto dei Ghiacciai Italiani, 4 Vol., CGI, Torino, 1959–1962.
Cogley, J. G.: Geodetic and direct mass-balance measurements: comparison and joint analysis, Ann. Glaciol., 50, 96–100, 2009.
DeBeer, C. M. and Sharp, M. J.: Topographic influences on recent changes of very small glaciers in the Monashee Mountains, British Columbia, Canada, J. Glaciol., 55, 691–700, 2009.
Desio, A.: I ghiacciai del Gruppo Ortles-Cevedale, Consiglio Nazionale delle Ricerche, Comitato Glaciologico Italiano, Milano, 875 pp., 1967.
De Woul, M. and Hock, R.: Static mass-balance sensitivity of Arctic glaciers and ice caps using a degree-day approach, Ann. Glaciol., 42, 217–224, 2005.

Diolaiuti, G., Maragno, D., D'Agata, C., Smiraglia, C., and Bocchiola, D.: Glacier retreat and climate change: documenting the last 50 years of Alpine glacier history from area and geometry changes of Dosdè Piazzi glaciers (Lombardy Alps, Italy), Progr. Phys. Geogr., 35, 161–182, 2011.
Dyurgerov, M. B. and Meier, M. F.: Glaciers and the Changing Earth System: A 2004 Snapshot, Occas. Pap., 58, Institute of Arctic and Alpine Research, University of Colorado, Boulder, 117 pp., 2005.
Dyurgerov, M., Meier, M. F., and Bahr, D. B.: A new index of glacier area change; a tool for glacier monitoring, J. Glaciol., 55, 710–716, 2009.
Elsberg, D. H., Harrison, W. D., Echelmeyer, K. A., and Krimmel, R. M.: Quantifying the effects of climate and surface change on glacier mass balance, J. Glaciol., 47, 649–658, 2001.
Ekstrand, S.: Landsat TM-based forest damage assessment: correction for topographic effects, Photogram. Eng. Rem. S., 62, 151–161, 1996.
Fischer, A.: Comparison of direct and geodetic mass balances on a multi-annual time scale, The Cryosphere, 5, 107–124, doi:10.5194/tc-5-107-2011, 2011.
Fountain, A. G., Hoffman, M. J., Granshaw, F., and Riedel, J.: The "benchmark glacier" concept – does it work? Lessons from the North Cascade Range, USA, Ann. Glaciol., 50, 163–168, 2009.
Frei, C. and Schär, C.: A precipitation climatology of the Alps from high-resolution rain-gauge observations, Int. J. Climatol., 18, 873–900, 1998.
Furbish, D. J. and Andrews, J. T.: The use of hypsometry to indicate long-term stability and response of valley glaciers to changes in mass transfer, J. Glaciol., 30, 199–211, 1984.
Gabrielli, P., Carturan, L., Gabrieli, J., Dinale, R., Krainer, K., Hausmann, H., Davis, M., Zagorodnov, V. S., Seppi, R., Barbante, C., Dalla Fontana, G., and Thompson, L. G.: Atmospheric warming threatens the untapped glacial archive of Ortles mountain, South Tyrol, J. Glaciol., 56, 843–853, 2010.
Gabrieli, J., Carturan, L., Gabrielli, P., Kehrwald, N., Turetta, C., Cozzi, G., Spolaor, A., Dinale, R., Staffler, H., Seppi, R., dalla Fontana, G., Thompson, L., and Barbante, C.: Impact of Po Valley emissions on the highest glacier of the Eastern European Alps, Atmos. Chem. Phys., 11, 8087–8102, doi:10.5194/acp-11-8087-2011, 2011.
Gabrielli, P., Barbante, C., Carturan, L., Cozzi, G., Dalla Fontana, G., Dinale, R., Dragà, G., Gabrieli, J., Kehrwald, N., Mair, V., Mikhalenko, V., Piffer, G., Rinaldi, M., Seppi, R., Spo-

laor, A., Thompson, L. G., and Tonidandel, D.: Discovery of cold ice in a new drilling site in the Eastern European Alps, Geogr. Fis. Din. Quat., 35, 101–105, 2012.

Gardelle, J., Berthier, E., and Arnaud, Y.: Impact of resolution and radar penetration on glacier elevation changes computed from DEM differencing, J. Glaciol., 58, 419–422, 2012.

Geist, T. and Stötter, J.: Documentation of glacier surface elevation change with multi-temporal airborne laser scanner data – case study: Hintereisferner and Kesselwandferner, Tyrol, Austria, Z. Gletscherkd. Glazialgeol., 41, 77–106, 2007.

Gerbaux, M., Genthon, C., Etchevers, P., Vincent, C., and Dedieu, J. P.: Surface mass balance of glaciers in the French Alps: distributed modeling and sensitivity to climate change, J. Glaciol., 51, 561–572, 2005.

GlobGlacier: Technical Specification (TS), GlobGlacier Deliverable 3, available at: http://www.globglacier.ch/docs/globgl_deliv3.pdf, 2008.

Haeberli, W., Hoelzle, M., Paul, F., and Zemp, M.: Integrated monitoring of mountain glaciers as key indicators of global climate change: the European Alps, Ann. Glaciol., 46, 150–160, 2007.

Haug, T., Rolstad, C., Elvehøy, H., Jackson, M., and Maalen-Johansen, I.: Geodetic mass balance of the western Svartisen ice cap, Norway, in the periods 1968–1985 and 1985–2002, Ann. Glaciol., 50, 119–125, 2009.

Hoelzle, M., Haeberli, W., Dischl, M., and Peschke, W.: Secular glacier mass balances derived from cumulative glacier length changes, Global Planet. Change, 36, 295–306, 2003.

Hughes, P. D.: Response of a Montenegro glacier to extreme summer heatwaves in 2003 and 2007, Geogr. Ann., 192, 259–267, 2008.

Huss, M., Bauder, A., and Funk, M.: Homogenization of long-term mass balance time series, Ann. Glaciol., 50, 198–206, 2009.

Joerg, P. C., Morsdorf, F., and Zemp, M.: Uncertainty assessment of multi-temporal airborne laser scanning data: a case study at an Alpine glacier, Remote Sens. Environ., 127, 118–129, 2012.

Klok, E. J. and Oerlemans, J.: Model study of the spatial distribution of the energy and mass balance of Morteratschgletscher, Switzerland, J. Glaciol., 48, 505–518, 2002.

Knoll, C. and Kerschner, H.: A glacier inventory for South Tyrol, Italy, based on airborne laser scanner data, Ann. Glaciol., 53, 46–52, 2009.

TCD
7, 267–319, 2013

Area and volume loss of the glaciers in the Ortles-Cevedale

L. Carturan et al.

Krimmel, R. M.: Mass balance and volume of South Cascade Glacier, Washington 1958 ± 1985, in: Glacier Fluctuations and Climate Change, edited by: Oerlemans, J., Kluwer Academic Publishers, Dordrecht, 193–206, 1989.

Krimmel, R. M.: Analysis of difference between direct and geodetic mass balance measurements at South Cascade Glacier, Washington, Geogr. Ann., 81, 653–658, 1999.

Kuhn, M.: The mass balance of very small glaciers, Z. Gletscherkd. Glazialgeol., 31, 171–179. 1995.

Kuhn, M., Markl, G., Kaser, G., Nickus, U., Obleitner, F., and Schneider, H.: Fluctuations of climate and mass balance: different responses of two adjacent glaciers, Z. Gletscherkd. Glazialgeol., 21, 409–416, 1985.

Kuhn, M., Abermann, J., Bacher, M., and Olefs, M.: The transfer of mass-balance profiles to unmeasured glaciers, Ann. Glaciol., 50, 185–190, 2009.

Kulkarni, A. V.: Mass balance of Himalayan glaciers using AAR and ELA methods, J. Glaciol., 38, 101–104, 1992.

Lambrecht, A. and Kuhn, M.: Glacier changes in the Austrian Alps during the last three decades, derived from the new Austrian glacier inventory, Ann. Glaciol., 46, 177–184, 2007.

Law, K. H. and Nichol, J.: Topographic correction for differential illumination effects on Ikonos satellite imagery, Proceedings of XXth ISPRS Congress: Geo-imagery bridging continents, Istanbul, Turkey, ISPRS, Vol. 35, Part 3B, 2004.

Machguth, H., Eisen, O., Paul, F., and Hoelzle, M.: Strong spatial variability of snow accumulation observed with helicopter-borne GPR on two adjacent Alpine glaciers, Geophys. Res. Lett., 33, L13503, doi:10.1029/2006GL026576, 2006.

Manley, W. F.: Geospatial inventory and analysis of glaciers: a case study for the eastern Alaska Range, in: Satellite Image Atlas of Glaciers of the World, edited by: Williams Jr, R. S. and J. G. Ferrigno, USGS Professional Paper 1386-K, United States Geological Survey, Denver, CO K424–K439, 2008.

Maragno, D., Diolaiuti, G., D'agata, C., Mihalcea, C., Bocchiola, D., Bianchi Janetti, E., Riccardi, A., and Smiraglia, C.: New evidence from Italy (Adamello Group, Lombardy) for analysing the ongoing decline of Alpine glaciers, Geogr. Fis. Din. Quat., 32, 31–39, 2009.

McFadden, E. M., Ramage, J., and Rodbell, D. T.: Landsat TM and ETM+ derived snowline altitudes in the Cordillera Huayhuash and Cordillera Raura, Peru, 1986–2005, The Cryosphere, 5, 419–430, doi:10.5194/tc-5-419-2011, 2011.

Minnaert, M.: The reciprocity principle in lunar photometry, Astrophys. J., 93, 403–410, 1941.

Nicholson, L. and Benn D. I.: Calculating ice melt beneath a debris layer using meteorological data, J. Glaciol., 52, 463–470, 2006.
Oerlemans, J.: Glaciers and Climate Change, Balkema Publishers, Lisse, 148 pp., 2001.
Østrem, G. and Brugman, M.: Glacier mass-balance measurements, a manual for field and office work, N.H.R.I. Science Report, 4, 224 pp., 1991.
Patzelt, G.: The period of glacier advances in the Alps, 1965 to 1980, Z. Gletscherkd. Glazialgeol., 21, 403–407, 1985.
Paul, F.: Correspondence. Calculation of glacier elevation changes with SRTM: is there an elevation dependent bias?, J. Glaciol., 54, 945–946, 2008.
Paul, F.: The influence of changes in glacier extent and surface elevation on modeled mass balance, The Cryosphere, 4, 569–581, doi:10.5194/tc-4-569-2010, 2010.
Paul, F. and Haeberli, W.: Spatial variability of glacier elevation changes in the Swiss Alps obtained from two digital elevation models, Geophys. Res. Lett., 35, L21502, doi:10.1029/2008GL034718, 2008.
Paul, F. and Kääb, A.: Perspectives on the production of a glacier inventory from multispectral satellite data in Arctic Canada: Cumberland Peninsula, Baffin Island, Ann. Glaciol., 42, 59–66, 2005.
Paul, F., Kääb, A., Maisch, M., Kellenberger, T. W., and Haeberli, W.: The new remote sensing-derived Swiss glacier inventory: I. Methods, Ann. Glaciol., 34, 355–361, 2002.
Paul, F., Kääb, A., Maisch, M., Kellenberger, T., and Haeberli, W.: Rapid disintegration of Alpine glaciers observed with satellite data, Geophys. Res. Lett., 31, L21402, doi:10.1029/2004GL020816, 2004.
Paul, F., Machguth, H., and Kääb, A.: On the impact of glacier albedo under conditions of extreme glacier melt: the summer of 2003 in the Alps, EARSeL Workshop on Remote Sensing of Land Ice and Snow, Berne, 21–23 February 2005, EARSeL eProceedings, 4, 139–149, CD-ROM, 2005.
Paul, F., Kääb, A., and Haeberli, W.: Recent glacier changes in the Alps observed by satellite: consequences for future monitoring strategies, Global Planet. Change, 56, 111–122, 2007a.
Paul, F., Maisch, M., Rothenbühler, C., Hoelzle, M., and Haeberli, W.: Calculation and visualization of future glacier extent in the Swiss Alps by means of hypsographic modelling, Global Planet. Change, 55, 343–357, 2007b.

Paul, F., Barry, R., Cogley, J. G., Frey, H., Haeberli, W., Ohmura, A., Ommanney, C. S. L., Raup, B., Rivera, A., and Zemp, M.: Recommendations for the compilation of glacier inventory data from digital sources, Ann. Glaciol., 50, 119–126, 2009.

Paul, F., Frey, H., and Le Bris, R.: A new glacier inventory for the European Alps from Landsat TM scenes of 2003: challenges and results, Ann. Glaciol., 52, 144–152, 2011.

Paul, F., and the Glaciers_cci Team: On the accuracy of glacier outlines derived from satellite data, Geophys. Res. Abstr., 14, EGU2012–12298, 2012.

Rabatel, A., Dedieu, J- P., Thibert, E., Letréguilly, A., and Vincent, C.: 25 years (1981–2005) of equilibrium-line altitude and mass-balance reconstruction on Glacier Blanc, French Alps, using remote-sensing methods and meteorological data, J. Glaciol., 54, 307–314, 2008.

Rastner, P., Bolch, T., Mölg, N., Machguth, H., Le Bris, R., and Paul, F.: The first complete inventory of the local glaciers and ice caps on Greenland, The Cryosphere, 6, 1483–1495, doi:10.5194/tc-6-1483-2012, 2012.

Rolstad, C., Haug, T., and Denby, B.: Spatially integrated geodetic glacier mass balance and its uncertainty based on geostatistical analysis: application to the western Svartisen ice cap, Norway, J. Glaciol., 55, 666–680, 2009.

Sapiano, J. J., Harrison, W. D., and Echelmeyer, K. A.: Elevation, volume and terminus changes of nine glaciers in North America, J. Glaciol., 44, 119–135, 1998.

Thibert, E., Blanc, R., Vincent, C., and Eckert, N.: Glaciological and volumetric mass-balance measurements: error analysis over 51 years for Glacier de Sarennes, French Alps, J. Glaciol., 54, 522–532, 2008.

Törmä, M. and Härmä, P.: Topographic correction of Landsat ETM-Images in Finnish Lapland, IEEE Int., 6, 3629–3631, 2003.

UNEP/WGMS: Global Glacier Changes: Facts and Figures, edited by: Zemp, M., Roer, I., Kääb, A., Hoelzle, M., Paul, F., and Haeberli, W., UNEP, World Glacier Monitoring Service, Zurich, Switzerland, 88 pp., 2008.

VanLooy, J. A. and Forster, R. R.: Use of historical elevation data to calculate surface-elevation and volume changes of Ha-Iltzuk Icefield, southwest British Columbia, Canada, 1970 to mid-1980s, Ann. Glaciol., 52, 109–115, 2011.

WGMS (World Glacier Monitoring Service): World Glacier Inventory – Status 1988, edited by: Haeberli, W., Bösch, H., Scherler, K., Østrem, G., and Wallén, C. C., IAHS (ICSI)/UNEP/UNESCO, World Glacier Monitoring Service, Zurich, Switzerland, 458 pp, 1989.

TCD

7, 267–319, 2013

Area and volume loss of the glaciers in the Ortles-Cevedale

L. Carturan et al.

WGMS (World Glacier Monitoring Service): Fluctuations of Glaciers 2000–2005, Vol. IX, edited by: Haeberli, W., Zemp, M., Kääb, A., Paul, F., and Hoelzle, M., ICSU (FAGS)/IUGG (IACS)/UNEP/UNESCO/WMO, World Glacier Monitoring Service, Zurich, Switzerland, 266 pp., 2008.
WGMS (World Glacier Monitoring Service): Glacier Mass Balance Bulletin No. 9 (2006–2007), edited by: Haeberli, W., Gartner-Roer, I., Hoelzle, M., Paul, F., Zemp, M., and ICSU (WDS)/IUGG (IACS)/UNEP/UNESCO/WMO, World Glacier Monitoring Service, Zurich, Switzerland, 96 pp., 2009.
WGMS (World Glacier Monitoring Service): Glacier Mass Balance Bulletin No. 11 (2008–2009), edited by: Zemp, M., Nussbaumer, S. U., Gärtner-Roer, I., Hoelzle, M., Paul, F., and Haeberli, W., ICSU (WDS)/IUGG (IACS)/UNEP/UNESCO/WMO, World Glacier Monitoring Service, Zurich, Switzerland, 102 pp., 2011.
Zanon, G.: Venticinque anni di bilancio di massa del ghiacciaio del Careser, 1966–67/1990–91, Geogr. Fis. Din. Quat., 15, 215–220, 1992.
Zemp, M.: Glaciers and Climate Change – Spatio-Temporal Analysis of Glacier Fluctuations in the European Alps after 1850, Ph.D. thesis, University of Zurich, 201 pp., 2006.
Zemp, M., Frauenfelder, R., Haeberli, W., and Hoelzle M.: Worldwide glacier mass balance measurements: general trends and first results of the extraordinary year 2003 in Central Europe, Data of Glaciological Studies, 99, 3–12, 2005.
Zemp, M., Hoelzle, M., and Haeberli, W.: Distributed modelling of the regional climatic equilibrium line altitude of glaciers in the European Alps, Global Planet. Change, 56, 83–100, 2007.
Zemp, M., Paul, F., Hoelzle, M., and Haeberli, W.: Glacier fluctuations in the European Alps 1850–2000: an overview and spatio-temporal analysis of available data, in: The Darkening Peaks: glacial Retreat in Scientific and Social Context, edited by: Orlove, B., Wiegandt, E. and B. Luckman, University of California Press, 152–167, 2008.
Zemp, M., Jansson, P., Holmlund, P., Gärtner-Roer, I., Koblet, T., Thee, P., and Haeberli, W.: Reanalysis of multi-temporal aerial images of Storglaciären, Sweden (1959–99) – Part 2: Comparison of glaciological and volumetric mass balances, The Cryosphere, 4, 345–357, doi:10.5194/tc-4-345-2010, 2010.

Table 1. Characteristics of the digital terrain models available for the Ortles-Cevedale group.

		DTM 1980s			DTM 2000s		
Province	Time interval (yr)	Acquisition date	Cell size (m)	Method	Acquisition date	Cell size (m)	Method
Sondrio and Brescia	26	19 Aug 1981	20	Aerial photogrammetry	Late summer 2007	5	Aerial photogrammetry
Trento	23	24 Sep 1983	10	Aerial photogrammetry	October 2006	2	LiDAR
Bolzano	21	Late summer 1984	20	Aerial photogrammetry	Late summer 2005	2.5	LiDAR

TCD
7, 267–319, 2013

TCD
7, 267–319, 2013

Table 2. Comparison of mean values of Accumulation Area Ratios from direct observations (decade 2000–2009) with the value obtained from the Landsat scene of 31 August 2009, for four glaciers of the Ortles-Cevedale group.

		Observed 2000–2009				2009 from Landsat	Difference (2009 from Landsat – mean 2000–2009 observed)
Glacier	Area km^2	Min	Max	Dev. St.	Mean		
La Mare (southern branch)	2.1	0.06	0.76	0.23	0.34	0.37	+0.03
Careser	2.1	0.00	0.12	0.04	0.01	0.06	+0.05
Fontana Bianca	0.5	0.00	0.95	0.30	0.12	0.24	+0.12
Rossa	0.9	0.07	0.72	0.20	0.31	0.43	+0.12
		Area-weighted mean			0.19	0.25	+0.06

Table 3. Change of key parameters in the Ortles-Cevedale glacier system from the 1980s to the 2000s.

	Statistics for all glaciers			Statistics for the 112 ice bodies remaining in 2009					
	1980s	2000s	Change	Change (count %)			Change		
				Negative	Positive	Unchanged	Min	Max	Mean
Area	100.3 km^2	76.8 km^2	−23.5 km^2 (−23.4 %)	100	–	–	−48 %	−6 %	−36 %
Debris cover	10.5 km^2	12.5 km^2	+2 km^2 (+19 %)	30	69	1	−67 %	+100 %	+8 %
Average elevation	3110 m	3124 m	+14 m	48	51	1	−121 m	+189 m	+5 m
Min-max elevation range	1795	1721	−74 m	92	7	1	−453 m	+40 m	−80 m
Average slope	21.7°	21.3°	−0.4°	44	56	–	−12°	+7°	+0°
Average clear-sky radiation	229.7 $W m^{-2}$	228.6 $W m^{-2}$	−1.1 $W m^{-2}$ (−0.5 %)	79	20	1	−27.1 $W m^{-2}$ (−11 %)	+14.3 $W m^{-2}$ (+8 %)	−5.9 $W m^{-2}$ (−3 %)

TCD
7, 267–319, 2013

Table 4. Area change of glaciers from 1987 to 2009, clustered for size classes.

Size class (km^2)	1987 count	1987 area (km^2)	2009 area (km^2)	Area change 2009–1987	
				km^2	%
< 0.1	38	2.03	0.72	−1.31	−64.5
0.1–0.5	54	12.92	7.52	−5.40	−41.8
0.5–1.0	15	10.39	7.83	−2.56	−24.6
1.0–5.0	24	55.34	44.04	−11.30	−20.4
5.0–10.0	1	6.79	5.45	−1.34	−19.7
> 10.0	1	12.81	11.26	−1.55	−12.1
Sum	133	100.28	76.82		
Area change				−23.46	−23.4

TCD
7, 267–319, 2013

Table 5. Correlation matrix for ten variables (79 glaciers in the lower left, 33 glacierets in the upper right).

	Mass budget	Elevation	Slope	Aspect	Clear sky radiation	AAR	Debris cover	Elevation range	Area	Avalanche ratio
Mass budget	1.00	−0.02	0.40[b]	0.06	−0.14	0.26	0.44[a]	0.17	−0.32[c]	0.44[a]
Elevation	0.27[b]	1.00	−0.24	0.65[a]	0.72[a]	0.36[b]	−0.55[a]	−0.14	−0.26	−0.16
Slope	0.43[a]	−0.08	1.00	−0.48[a]	−0.73[a]	−0.16	0.47[a]	0.66[a]	0.28	0.23
Aspect	−0.01	0.56[a]	−0.24[b]	1.00	0.86[a]	0.35[b]	−0.37[b]	−0.19	−0.36[b]	0.19
Clear sky radiation	−0.10	0.72[a]	−0.61[a]	0.78[a]	1.00	0.33[c]	−0.46[a]	−0.49[a]	−0.43[b]	0.03
AAR	0.43[a]	0.50[a]	0.02	0.07	0.17	1.00	−0.48[a]	0.07	−0.12	0.29[c]
Debris cover	0.10	−0.46[a]	0.39[a]	−0.01	−0.39[a]	−0.43[a]	1.00	0.11	0.00	0.40[b]
Elevation range	0.42[a]	−0.01	0.11	−0.08	−0.17	0.42[a]	−0.02	1.00	0.60[a]	0.25
Area	0.04	0.08	−0.32[a]	−0.03	0.14	0.34[a]	−0.29[a]	0.58[a]	1.00	−0.02
Avalanche ratio	0.21[c]	−0.21[c]	0.45[a]	0.16	−0.22[c]	−0.22[c]	0.71[a]	0.06	−0.26[b]	1.00

Correlations significant at the 0.01, 0.05 and 0.10 levels are marked with [a], [b] and [c], respectively.

TCD
7, 267–319, 2013

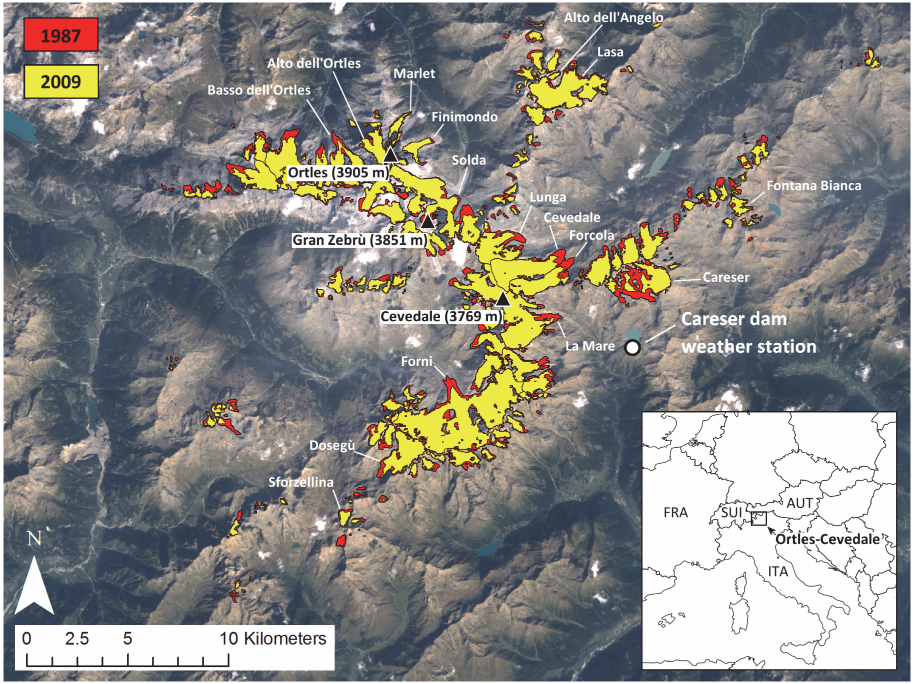

Fig. 1. Geographic setting of the Ortles-Cevedale group with glacier extents from 1987 and 2009. Named glaciers are referred to in the text.

TCD
7, 267–319, 2013

Area and volume loss of the glaciers in the Ortles-Cevedale

L. Carturan et al.

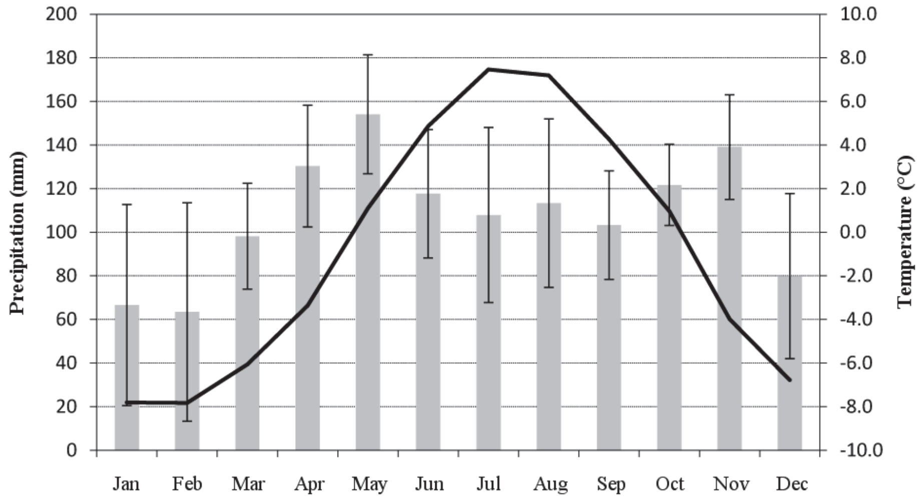

Fig. 2. Monthly air temperature (line) and precipitation (histogram) at the Careser dam weather station (2605 m a.s.l.), averaged over the period 1959–2009. Bars on histogram indicate one standard deviation.

TCD
7, 267–319, 2013

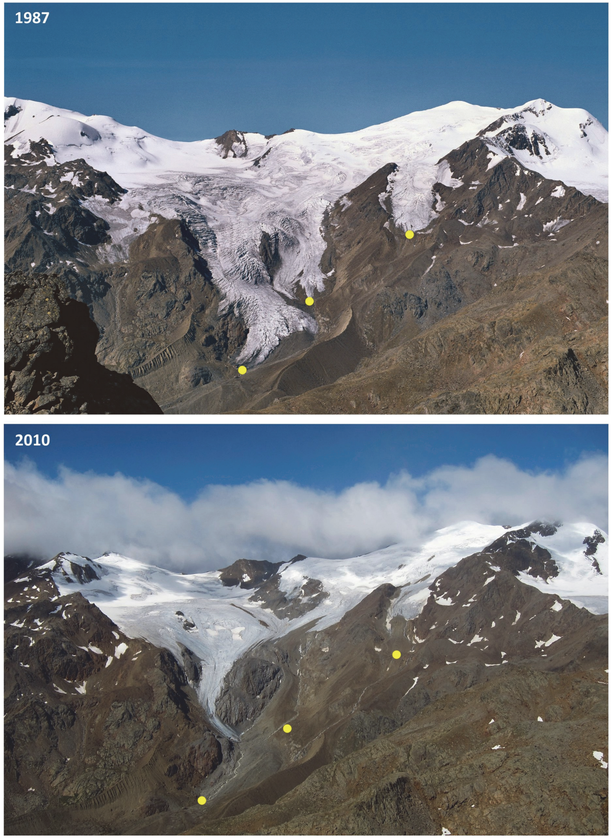

Fig. 3. Example of the current shrinking of glaciers in the Ortles-Cevedale group. Repeat photography of La Mare Glacier in late summer 1987 (photo Giuliano Bernardi, www.fotobernardi.it) and on 28 August 2010 (photo L. Carturan).

TCD
7, 267–319, 2013

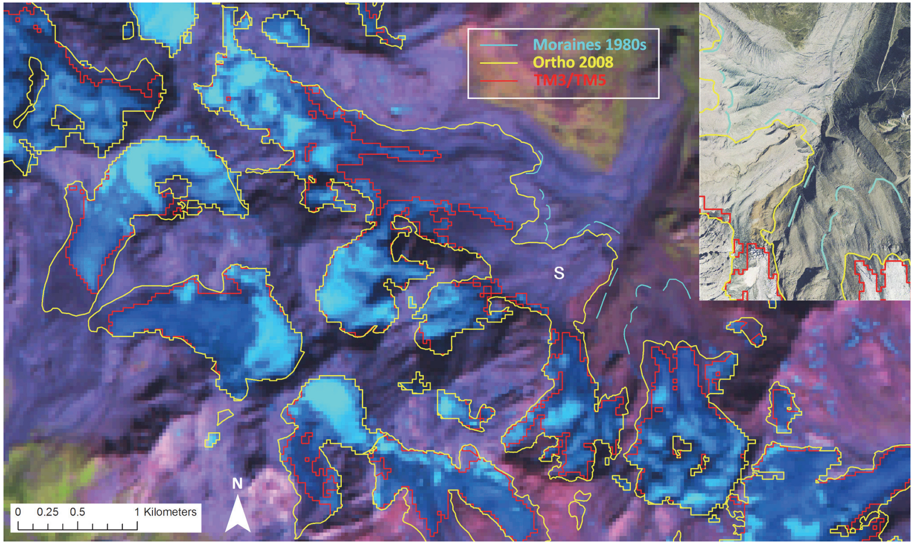

Fig. 4. Comparison of the automatic delineation of Solda Glacier (S) from the thresholded band ratio image of 31 August 2009 (TM3/TM5; RGB composite of bands 5, 4, and 3 in the background) and post-processed delineation from aerial orthophoto (ortho 2008, in the inset). Lateral and terminal moraines built by this glacier in the mid 1980s (in light blue) were used for post-processing the automatic delineation from the 1987 Landsat image.

TCD
7, 267–319, 2013

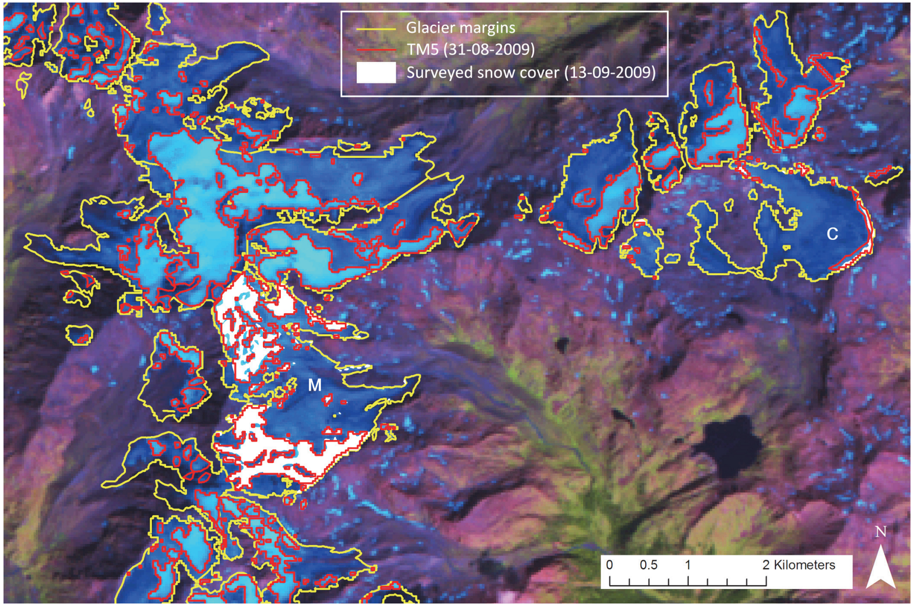

Fig. 5. Comparison of snow cover mapping from ground surveys (white areas) and from Landsat (TM5, red line) at the end of the 2009 ablation season on La Mare (M) and Careser (C) glaciers. The background image is a composite with Landsat bands TM 5, 4, and 3 as RGB.

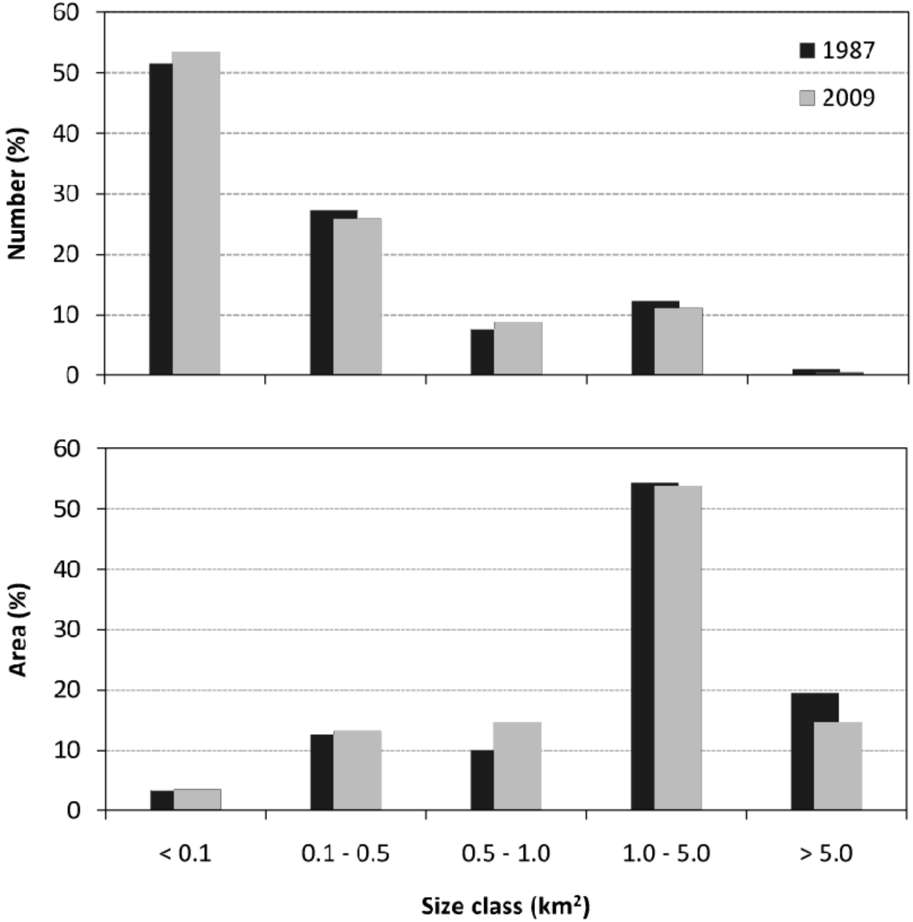

Fig. 6. Bar graphs showing percentages of glacier number and area per size classes.

TCD
7, 267–319, 2013

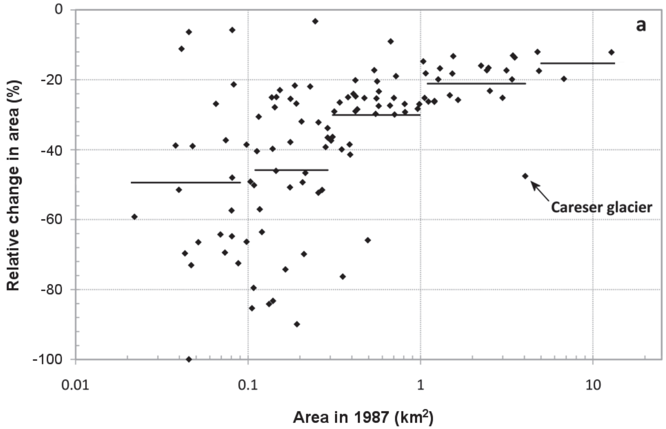

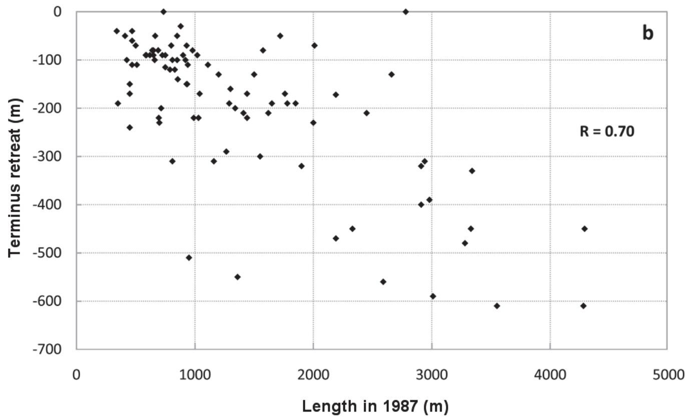

Fig. 7. Relative change in area vs. initial area in 1987 **(a)** and terminus retreat vs. initial length in 1987 **(b)**. Horizontal lines in **(a)** show mean values for size classes.

TCD
7, 267–319, 2013

Area and volume loss of the glaciers in the Ortles-Cevedale

L. Carturan et al.

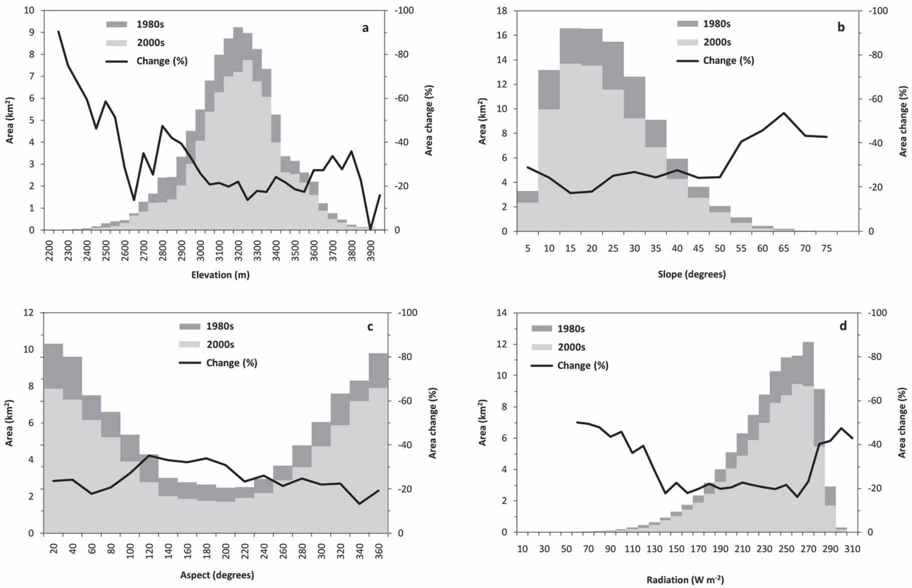

Fig. 8. Area distribution of the Ortles-Cevedale glaciers from 1987 to 2009 and percent change for classes of **(a)** elevation, **(b)** slope, **(c)** aspect, and **(d)** summer clear-sky radiation.

TCD

7, 267–319, 2013

Area and volume loss of the glaciers in the Ortles-Cevedale

L. Carturan et al.

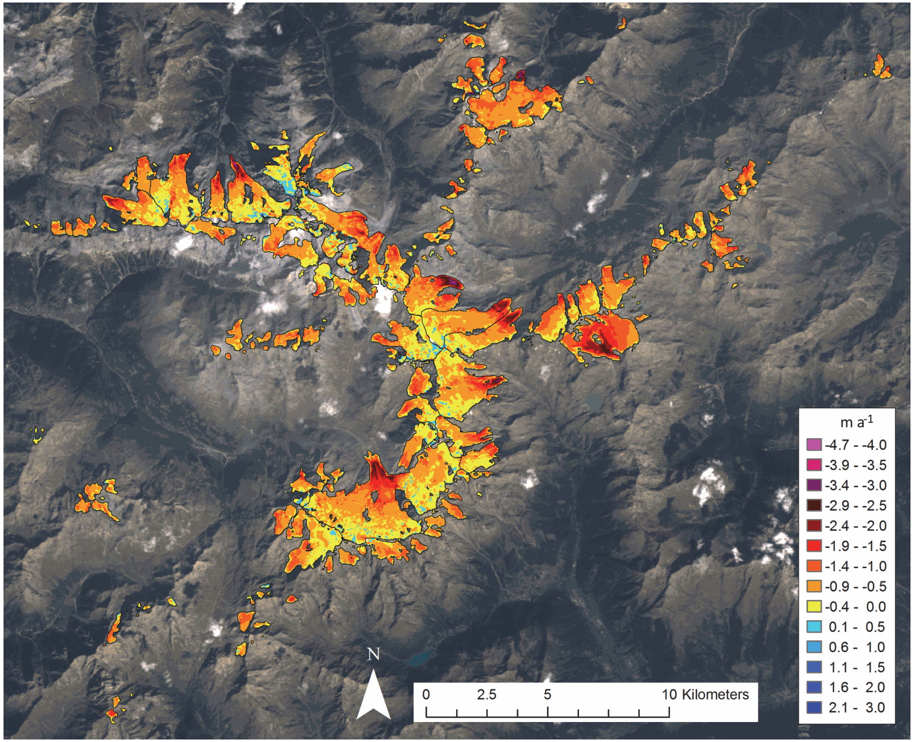

Fig. 9. Mean annual elevation change rates of the Ortles-Cevedale glaciers from the 1981–1984 period to the 2005–2007 period.

TCD
7, 267–319, 2013

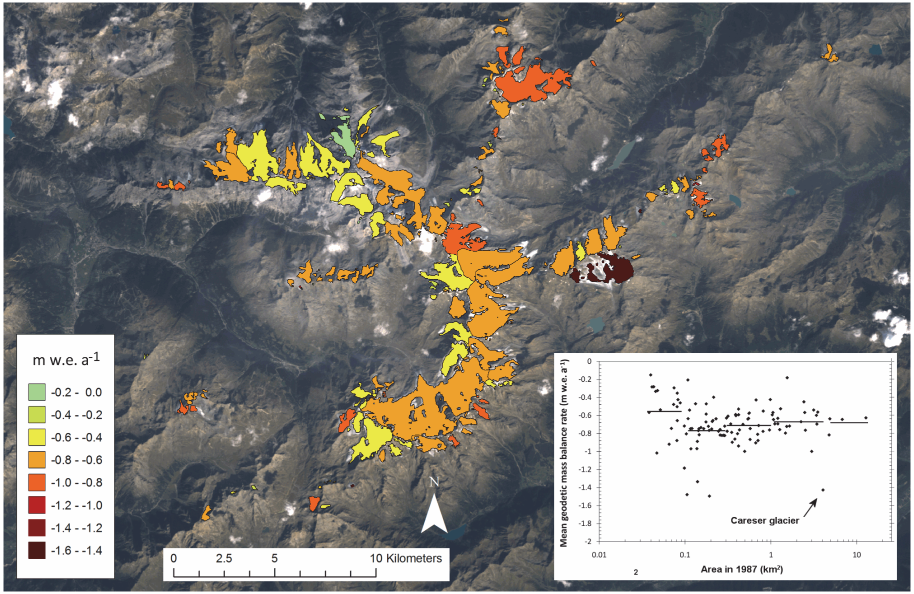

Fig. 10. Glacier specific mean geodetic mass balance rates over the same periods as in Fig. 9. The scatterplot shows the values plotted vs. initial area in 1987.

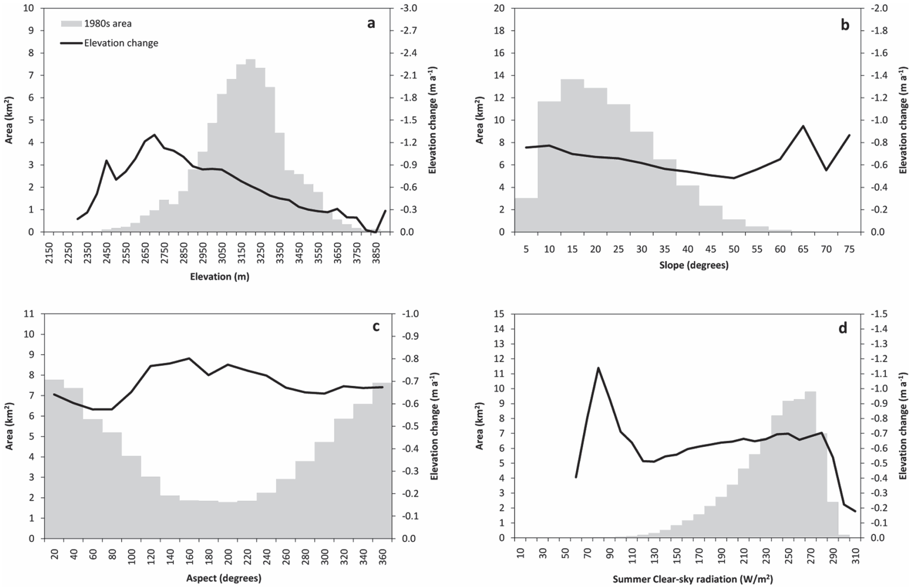

Fig. 11. Elevation changes of the Ortles-Cevedale glacier system from the 1980s to the 2000s, for classes of **(a)** elevation, **(b)** slope, **(c)** aspect and **(d)** summer clear-sky radiation. The area distribution in the 1980s is shown to give a background for the reported elevation changes.

TCD

7, 267–319, 2013

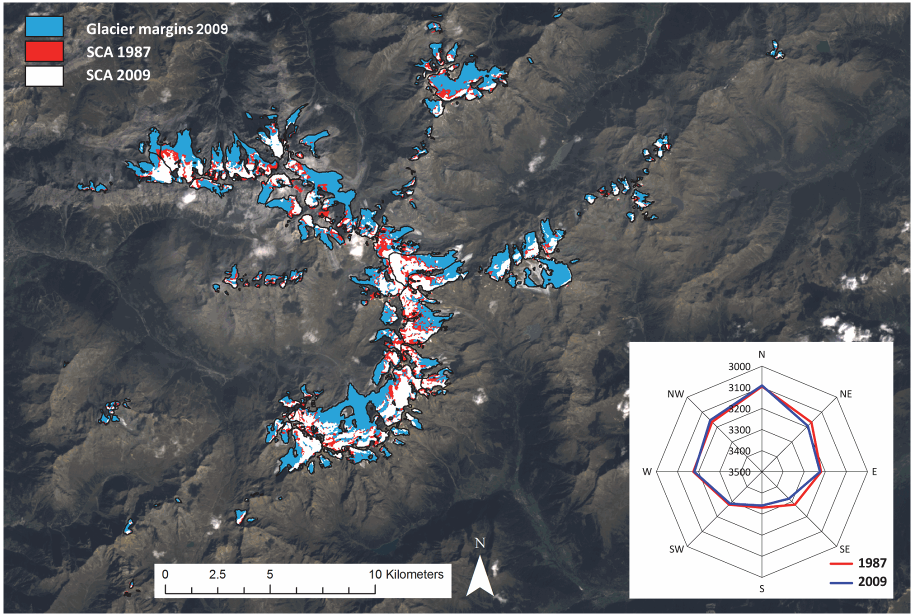

Fig. 12. Snow covered area in the late summer of 1987 (red and white) and 2009 (white only). The radar chart shows the snow line altitude versus main aspect direction in both years.

TCD
7, 267–319, 2013

Area and volume loss of the glaciers in the Ortles-Cevedale

L. Carturan et al.

Title Page
Abstract
Introduction
Conclusions
References
Tables
Figures
◀
▶
Back
Close
Full Screen / Esc
Printer-friendly Version
Interactive Discussion

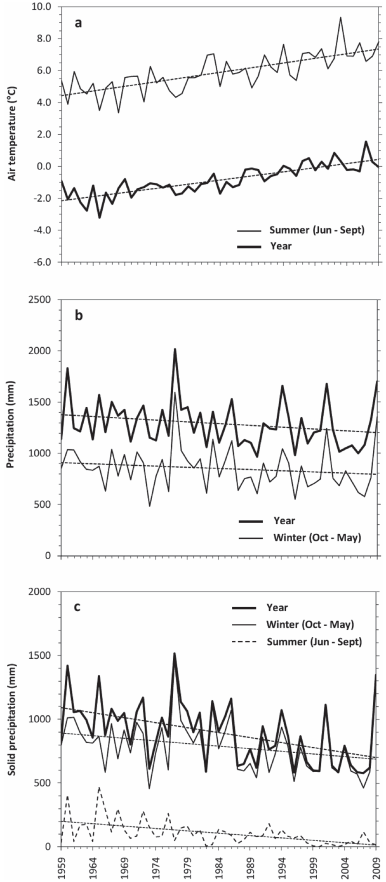

Fig. 13. Time series of meteorological observations from 1959 to 2009 at the Careser dam weather station (2605 m a.s.l.): **(a)** air temperature; **(b)** total precipitation; **(c)** solid precipitation.

TCD
7, 267–319, 2013